

co2amp 2020

Mikhail Polyanskiy

November 4, 2021

Contents

| | | |
|----------|--|-----------|
| 1 | General notes | 3 |
| 1.1 | Program capabilities | 3 |
| 1.2 | Availability, tools and third party components | 4 |
| 1.3 | Acknowledgements | 4 |
| 2 | Basic concepts | 5 |
| 2.1 | co2amp and co2am+ | 5 |
| 2.2 | Projects | 5 |
| 2.3 | Pulse, layout and optic | 5 |
| 2.4 | Calculation grid | 6 |
| 2.5 | Units | 7 |
| 2.6 | Program output | 7 |
| 2.7 | "Comments" and "About" tabs of co2am+ | 8 |
| 3 | Elements of a project | 10 |
| 3.1 | Pulse | 10 |
| 3.2 | Layout | 11 |
| 3.2.1 | Configuration | 11 |
| 3.2.2 | Dealing with long optical elements | 11 |
| 3.2.3 | Modelling of pulse propagation between optics | 12 |
| 3.3 | Optic type A <i>Active medium</i> | 14 |
| 3.4 | Optic type P <i>Probe</i> | 15 |
| 3.5 | Optic type F <i>Spatial filter</i> | 15 |
| 3.6 | Optic type S <i>Spectral filter</i> | 15 |
| 3.7 | Optic type L <i>Lens</i> | 16 |
| 3.8 | Optic type M <i>Material</i> | 16 |
| 3.9 | Optic type C <i>Chirper</i> | 18 |
| 4 | Modelling of processes in CO₂ amplifiers | 19 |
| 4.1 | Molecular dynamics | 19 |
| 4.1.1 | Pumping by electric discharge | 19 |
| 4.1.2 | Pumping and vibrational relaxation dynamics | 20 |
| 4.1.3 | Optical pumping | 21 |
| 4.2 | Amplification | 22 |
| 4.2.1 | Laser transitions | 22 |
| 4.2.2 | Main equations | 22 |
| 4.2.3 | Populations | 24 |
| | Appendices | 26 |

| | |
|--|----|
| A Cross-sections of excitation processes | 27 |
| B Molecular constants | 31 |
| C Properties of optical materials | 39 |
| D Selected formulas explained | 42 |

Chapter 1

General notes

1.1 Program capabilities

1. Ultrashort pulse amplification in CO₂ active medium
 - Rotational numbers up to $J = 60$
 - Regular, hot and sequence bands
 - Isotopic CO₂
2. Molecular dynamics
 - Realistic pumping
 - Collisional relaxation processes
 - Stimulated transitions
 - Independent consideration of active medium regions at different elongations from the optical axis
3. Diffraction-based beam propagation
 - Beam manipulation with common optical elements
 - Arbitrary optical configurations
4. Linear dispersion and non-linear effects in optical materials
 - Pulse chirping
 - Kerr lensing
 - Self-phase modulation
5. Advanced optics
 - Chirped-pulse amplification
 - Spectral filtering
 - Trains of pulses
 - Staging (program output as an input for the next stage)
6. User's interface
 - Easy specification of parameters
 - Graphical output
 - Project save/recall

1.2 Availability, tools and third party components

The simulation core **co2amp** and the user's interface shell **co2am+** are written in C++ programming language. **co2am+** uses the QT library (<http://qt.io>), and QT Creator (a part of the QT project) is used as a development environment. Windows executables are built using the MinGW compiler obtained as a part of the open-source QT distribution. The code is published in the GitHub website (<https://github.com/polyanskiy/co2amp>) and is freely available for use, modification, and redistribution under the terms of the GNU General Public License (GPL v.3) (<https://www.gnu.org/licenses/gpl-3.0.html>). A binary package is provided in the form of a Windows installer that contains pre-compiled executables, documentation, templates and examples at <https://github.com/polyanskiy/co2amp/releases/>. The project only uses cross-platform libraries and thus should compile under other platforms (MacOS, Linux). **co2amp** depends on three third party components: gnuplot, 7-zip and HDF5 that are freely available for multiple platforms at <http://www.gnuplot.info/>, <https://www.7-zip.org/> and <https://www.hdfgroup.org/solutions/hdf5/> respectively. These components must be installed separately. The windows installer is built using the Nullsoft Scriptable Install System (NSIS, <https://nsis.sourceforge.io/>), and this is the only platform-specific part of the project. Finally, the documentation is mostly written in L^AT_EX (<http://www.latex-project.org>) using the Overleaf online editor and compiler (<https://www.overleaf.com/>). YAML and HDF5 file formats are adopted for the specification of input parameters and storing the output field information respectively.

1.3 Acknowledgements

Viktor Platonenko from Moscow State University (Russia) provided a **Mathcad** code for pulse amplification in the CO₂ active medium that was used as the starting point for developing the **co2amp** program; Dr. Platonenko also offered valuable input in the early stages of the work.

Chapter 2

Basic concepts

2.1 co2amp and co2am+

co2amp is a terminal program that allows simulating propagation of ultrashort pulses through an arbitrary cylindrically-symmetric optical system that can include CO₂ amplifiers. It takes inputs in the form of specially formatted text files and command line arguments and produces outputs in the form of tabulated data files and a binary file with the complete information on the output field. **co2amp** can be used independently, however a graphical user interface makes the task of managing the program's inputs and outputs much more convenient.

co2am+ is a graphical user interface program that simplifies the process of working with multiple input- and output- files and calculation parameters by keeping them organized and easily accessible via an intuitive working environment. **co2am+** allows saving/recalling the entire file structure of a project and command line parameters in a single compressed '.co2' file.

2.2 Projects

The **co2amp** input parameters include the characteristics of the initial **pulse(s)**, the optical **layout** configuration, specifications for all **optics** used in the model (including laser amplifiers), and calculation parameters (e.g. calculation grid definition).

The temporal shape of the pulse and the beam profile at every element of the optical layout are saved and can be accessed in both graphical and tabulated-numerical representations.

All **co2amp** inputs and outputs for a certain model constitute a project.

co2am+ allows storing all inputs and outputs of the model except the output field in a single compressed project file with a '.co2' extension. Complete pulse information (complex field in every node of the space-time calculation grid) at the output of the system can be saved separately as a binary HDF5 file ('.pulse' extension) and used as an input for another project. An example of the input file structure of a '.co2' project accessed via the **co2am+** interface is shown in Fig. 2.1.

2.3 Pulse, layout and optic

A **pulse** is a complex electric field defined in every node of the calculation grid. A project can include one or more input pulses. Each one of them is defined in a separate YAML ('.yaml') file. Either a reference to an output from another project (a '.pulse' file) or an explicit specification of the pulse's spatial- and temporal-profile can be used to define an input pulse.

The optical **layout** consists of a series of infinitely-thin **optics** separated by free space. **Pulses** propagate freely between the **optic**. A project must have one and only one **layout**. The **layout** is defined in a '.yaml'

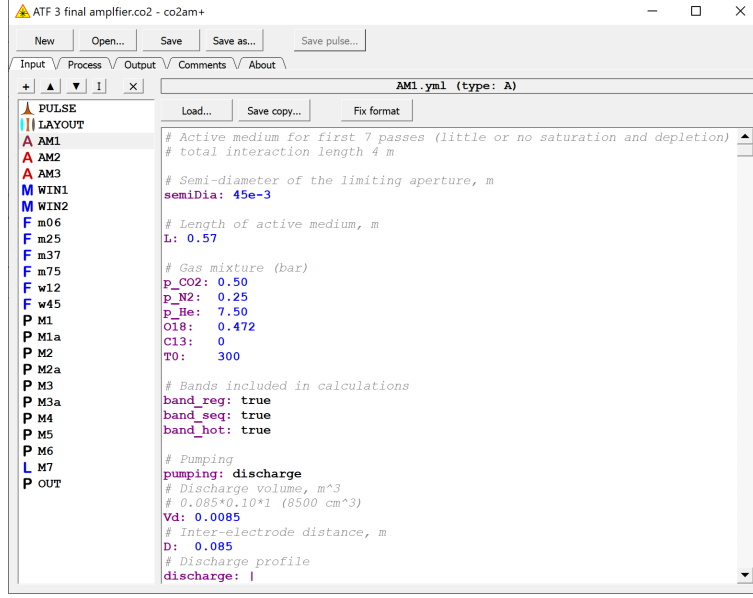


Figure 2.1: "Input" tab of the **co2am+** user interface program. YAML files specifying the **pulse**, **layout** and **optics** are listed on the left. Content of a selected file is displayed and can be edited in the big edit box on the right.

file that specifies the order of the **planes** and distances between them.

An **optic** is an element of a system that alters the pulse when it passes through it. There are several types of **optic** described in some detail later. For example, a *Lens* is an **optic** that introduces a radial-coordinate-dependent frequency shift changing the divergence of the beam. Each **optic** is specified in a separate '.yml' file. One **optic** can be used several times in the same **layout**. In this case **pulses** pass through the **optic** several times as, for example, in a laser cavity¹.

co2amp supports seven types of **optics** listed in the Table 2.1

2.4 Calculation grid

The **pulse** is defined as a complex electric field in the nodes of a 2-dimensional space-time calculation grid moving with the pulse. Calculation grid is mostly defined via **co2amp** command line arguments. The only exception is the maximum radial coordinate that is equal to the semi-diameter of the clear aperture of an **optic** and thus changes from **optic** to **optic**. The command line arguments associated with the pulse space-time calculation grid are the numbers of nodes ("precision") in the pulse time- and radial coordinate-grids, minimum- and maximum- time limits and the central frequency. The central frequency is needed to unambiguously define the calculation grid in the frequency domains.

Pulse time frame is used for all **pulse** related calculations (interaction with **optics**, free-space propagation) and for fast processes in some **optics**, e.g. fast molecular dynamics (stimulated transitions and rotational relaxation in an *Active medium*). Processes that are much slower than the duration of the pulse (e.g. pumping of the active medium and vibrational relaxation) are modeled separately in a slower laboratory time-frame. Time-tick of the laboratory time-frame is also defined via a **co2amp** command line argument.

In **co2am+** the **co2amp** command line arguments are specified in the "Process" tab (Fig. 2.2). The number of nodes in both coordinates of the pulse space-time frame always is a power of two that allows the

¹Internally, **co2amp** code uses an additional concept: a **plane**. A **plane** is an element of a **layout** that, unlike an **optic**, only appears in the **layout** once. An **optic** is then associated with each **plane**. A **plane** is basically a placeholder for an **optic**.

Table 2.1: Types of optics

| <i>Type ID</i> | <i>Name</i> | <i>Description</i> |
|----------------|------------------------|--|
| A | <i>Active medium</i> | A CO ₂ amplifier section. |
| P | <i>Probe</i> | A passive surface. May be used as a limiting aperture. |
| F | <i>Spatial filter</i> | An optic with coordinate-dependent transmission. |
| S | <i>Spectral filter</i> | An optic with frequency-dependent transmission. |
| L | <i>Lens</i> | An ideal thin lens. |
| M | <i>Material</i> | A layer of a material. May introduce linear- and/or non-linear dispersion and/or absorption. |
| C | <i>Chirper</i> | An optic that applies a chirp to the pulse. Typically stretcher or compressor. |

use of Fast Fourier Transform (FFT) algorithms. Calculations with a larger number of nodes usually are more accurate but, on the other hand, take longer and require more computer memory (both calculation time and required memory are roughly proportional to the product of the number of nodes in the time and space grids). Therefore it is recommended to start running the simulation with a smaller number of nodes and then repeat it several times, each time with a denser grid. The absence of considerable change in the program's output with an increase in the number of nodes will indicate that the density of the grid is satisfactory.

The time-step, $\Delta t = (t_{max} - t_{min})/N_t$, where t_{max} and t_{min} define the time range and N_t is the number of nodes in the time grid, must be small enough to accurately describe the pulse profile at all stages of its propagation through the optical system. It also is important to remember that the time range and number of nodes in the time grid also define the range and step in the frequency domain: $\Delta\nu = 1/(t_{max} - t_{min})$ and $(\nu_{max} - \nu_{min}) = 1/\Delta t$. This means that the time range must be long enough to provide sufficient resolution in the frequency domain, while, concurrently, the time step must be sufficiently short to provide a bandwidth that fits the entire spectral region of interest.

Identifying an appropriate calculation grid is very important for building an accurate model of an optical system. Putting an effort in this part of the simulation process will pay off with fast, reliable calculations.

2.5 Units

SI units without prefixes, e.g. "meters, seconds, Amperes..." but not "centimeters, nanoseconds, kiloamperes...", are used in **co2amp** input and output and also in the **co2amp** code internally. **co2amp+** allows changing the units used for the graphical representation of the calculation results on the "Output" tab (Fig. 2.3). However, when numerical data are accessed via [Right-click on a plot] – [Copy raw data] the units of the data are always "prefix-less".

2.6 Program output

The output of the program is given as a temporal and spatial structure of every **pulse** at each **optic** in the **layout**. Temporal (and spectral) profiles are integrated on the entire area of the **optic**, and spatial profiles are integrated on the duration of the pulse time-frame.

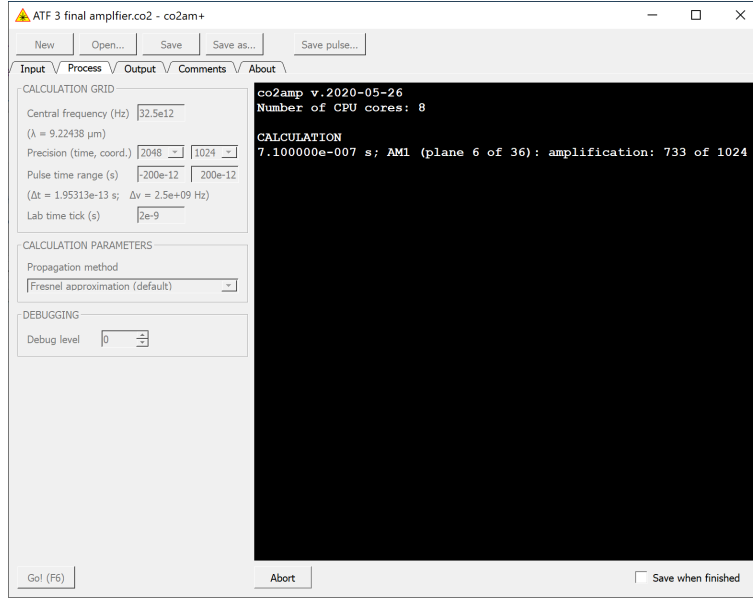


Figure 2.2: "Process" tab of the **co2am+** user interface program. Values of **co2amp** command line arguments are specified on the left. **co2amp** output is displayed in the black text box on the right.

In the **co2am+** "Output" tab the user can chose a **pulse** and an **optic** to display (Fig. 2.3). If the selected **optic** is used several times in the **layout**, it also is possible to specify which passes through the **optic** will be displayed. Also, the integral pulse energy can be provided either at every pass through a selected **optic**, or at all passes through all **optics** of the **layout**.

Output for some types of **optics** supplies additional type-specific information. For instance, for *Active medium*, this includes gain, discharge profile, population dynamics, and the dynamics of the distribution of pumping energy (fractions of discharge energy going into the excitation of laser levels, excitation of molecular translations and ionization). Output for the optic of type *Probe* include the information of the phase of the optical field in the center of the beam.

2.7 "Comments" and "About" tabs of co2am+

The "Comments" tab provides an edit box to enter any comments about the project that will be stored as a part of the project in the '.co2' file.

The "About" tab contains information about the versions of the **co2amp** and **co2am+** programs, links to the license and the documentation (this file), author contact information, and a suggested citation format.

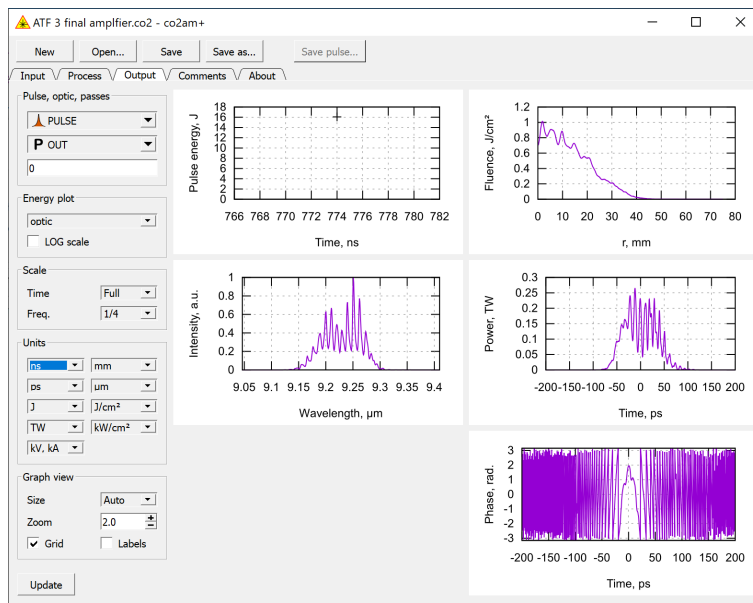


Figure 2.3: "Output" tab of the **co2am+** user interface program. Controls on the left allow selecting the data to display and fine-tuning the look of the plots.

Chapter 3

Elements of a project

A project must include the following elements specified in the input YAML files:

1. One or more **pulses**
2. One or more **optics**
3. One **layout**

Each element is specified in a dedicated YAML (‘.yaml’) file¹. The last **optic** in the **layout** must be of type **P** (*Probe*).

In the following sections we briefly describe each of these elements and discuss models associated with them. This description is not complete. Refer to the templates and the example files (and the comments in them) for more information.

3.1 Pulse

Unless the output of another project (‘.pulse’ file) is used as an input, both the temporal- and spatial- shape of the input **pulse** must be specified in a corresponding YAML (‘.yaml’) file. The **pulse** is assumed to be transform-limited (no initial chirping). The **pulse** energy, central frequency, and the injection time must also be specified. The injection time specifies the time-delay between the zero moment of the lab time frame (‘slow’ time frame) and injecting a **pulse** into the optical system (first **optic** in the **layout**). An example of a **pulse** configuration file is shown below.

```
#=====
# PULSE.yaml from 'examples/00 simple propagation.co2' project

t_in: 0
E: 1e-3
freq: 32.5e12

beam: GAUSS
w: 3e-3

pulse: GAUSS
fwhm: 2e-12
#=====
```

¹**co2amp** also requires an additional input file ‘config_files.yaml’ that lists all input YAML files and the types of corresponding elements. **co2am+** creates this file automatically.

This file specifies a 2 ps (FWHM) transform-limited Gaussian pulse with an $w = 3$ mm Gaussian beam profile, 1 mJ energy and 32.5 THz central frequency injected into the system at $t_{in} = 0$. There are several pre-defined beam- and pulse-profile options: **GAUSS**, **FLATTOP**, **SUPERGAUSS4**, **SUPERGAUSS6** etc. Alternatively, a **FREEFORM** option can be selected followed by a tabulated numerical specification of an arbitrary shape (see 'pulse.yml' template for details).

3.2 Layout

3.2.1 Configuration

The **layout** configuration defines the order of **optics** and the distances between them. A simple **layout** configuration file looks like this:

```
#=====
# LAYOUT.yml from 'examples/00 simple propagation.co2' project

- go: P1 >> 3 >> P2
  times: 1
#=====
```

Here, the system consists of two **optics**: P1 and P2 separated by 3 meters of free space. The pulse(s) pass through the system once. If the **times** value is more than 1, a pulse after passing through P2 will go to P1 again, and the propagation through the system will repeat the specified number of times. There can be several "go-times" in a **layout** configuration file. An example of a **layout** configuration for a more complex system is shown below

```
#=====
# LAYOUT.yml from 'examples/ATF 5 TW/ATF 1 regen.co2' project

- go: str >> COU1
  times: 1

- go: 0.45 >> i >> 0.90 >> GE >> 0.25 >> w >> WIN1 >> w >> 0.45 >> AM1 >> 0.40 >> AM2 >> 0.45
>> w >> WIN2 >> w >> 0.10 >> MIR >> m >> 0.10 >> w >> WIN2 >> w >> 0.45 >> AM2 >> 0.40 >> AM1
>> 0.45 >> w >> WIN1 >> w >> 0.25 >> GE >> 0.90 >> i >> 0.45 >> COU2
  times: 15

- go: 0.45 >> i >> 0.90 >> GE >> 0.25 >> w >> WIN1 >> w >> 0.45 >> AM1 >> 0.40 >> AM2 >> 0.45
>> w >> WIN2 >> w >> 0.10 >> MIR >> m >> 0.10 >> w >> WIN2 >> w >> 0.45 >> AM2 >> 0.40 >> AM1
>> 0.45 >> w >> WIN1 >> w >> 0.25 >> OUT
  times: 1
#=====
```

3.2.2 Dealing with long optical elements

In the **co2amp** model, the **optics** are infinitely thin. In a case of a long **optic**, for example an *Active medium*, the model first calculates the field modification accumulated by a **pulse** when it propagates through the **optic** and then apply it as if it occurred at once. This approach may not work well if the actual optical element is long and the **pulse** changes considerably while propagating through it, thus interacting differently with different parts of the **optic**. Accuracy of the model can be improved if long elements are divided into shorter sub-sections.

Fig. 3.1 shows an example of a 2-meter long layout with a meter long active medium in the middle. In one case shown in Fig. 3.1a we first propagate the pulse to the middle of the amplifier section, then apply the amplification accumulated over 1 meter and propagate the pulse to the last optic. The corresponding

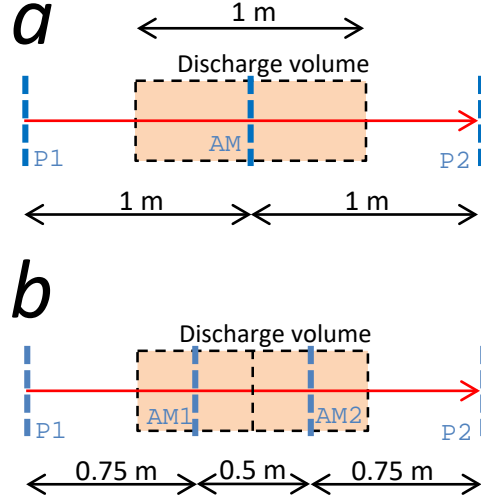


Figure 3.1: Example of layout configuration for a long optic (in this case an *Active medium*. a) The *Active medium* is represented by a single optic. b) The *Active medium* is split in two shorter sections.

layout configuration is

```
#####
# long amplifier
- go: P1 >> 1 >> AM >> 1 >> P2
  times: 1
#####
```

Alternatively, we can represent the active medium by two 0.5-meter sections as shown in Fig. 3.1b. The corresponding layout is

```
#####
# long amplifier is divided in two shorter sections
- go: P1 >> 0.75 >> AM1 >> 0.5 >> AM2 >> 0.75 >> P2
  times: 1
#####
```

Population dynamics in all amplifier sections is modeled separately, and thus, by splitting a long amplifier into shorter sections we also obtain a more realistic model of the active medium.

3.2.3 Modelling of pulse propagation between optics

Consider free-space wave propagation between plane-parallel surfaces S' and S separated by distance z as shown in Fig. 3.2 for the case of cylindrical symmetry. According to Huygens-Fresnel principle, the field E in a point on the plane S is defined as a superposition of secondary waves emitted from every point of plane

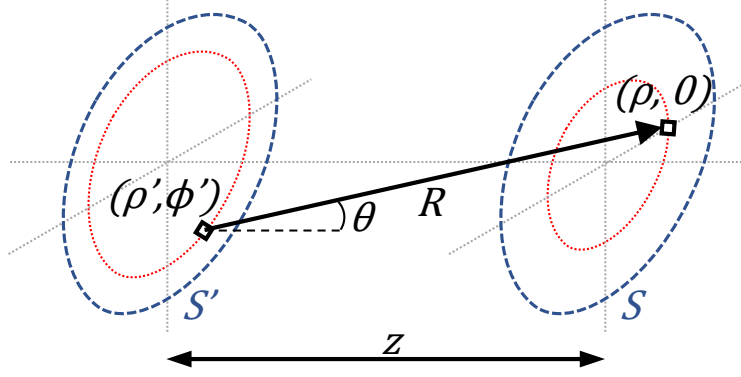


Figure 3.2: Application of Huygens-Fresnel principle to beam propagation from plane S' to plane S for a system with cylindrical symmetry.

S' [1]. This can be written in the case of cylindrical symmetry as [2, 3]

$$E(\rho) = -\frac{i}{\lambda} \int_{\rho'=0}^{\infty} E'(\rho') \int_{\phi'=0}^{2\pi} \frac{e^{ikR}}{R} K d\phi' \rho' d\rho' \quad (3.1a)$$

$$R = \sqrt{\rho^2 + \rho'^2 + z^2 - 2\rho\rho' \cos \phi'} \quad (3.1b)$$

$$K = \cos \theta = \frac{z}{R} \quad (3.1c)$$

where λ is the wavelength, $k = 2\pi/\lambda$ the wavenumber, and K the obliquity factor as it appears in Rayleigh-Sommerfeld diffraction theory.

Note that because the field on the output plane S doesn't depend on the angular coordinate ϕ , $\phi = 0$ is chosen for the simplification of Eq. (3.1).

Direct numerical integration of Eq. (3.1) having $O(N^3)$ complexity is very time consuming and thus an approximation is usually used to accelerate computations. Fresnel diffraction is the most known approximation to the diffraction integral. The following assumptions are done in the Fresnel approximation

$$K \approx 1$$

$$R \approx \begin{cases} z & \text{(denominator)} \\ z \left(1 + \frac{\rho^2 + \rho'^2 - 2\rho\rho' \cos \phi'}{2z^2} \right) & \text{(exponent)} \end{cases} \quad (3.2)$$

where "denominator" and "exponent" signify the position of the R variable in Eq. (3.1a).

After substituting Eq. (3.2) to Eq. (3.1a) and using the following formula

$$\int_0^{2\pi} e^{\pm ia \cos \phi} d\phi = 2\pi J_0(a) \quad (3.3)$$

where J is the Bessel function we get the expression for Fresnel diffraction with cylindrical symmetry

$$E(\rho) \approx -\frac{2\pi i e^{ik(z + \frac{k\rho^2}{2z})}}{\lambda z} \int_0^{\infty} E'(\rho') e^{i\frac{k\rho'^2}{2z}} J_0\left(\frac{k\rho\rho'}{z}\right) \rho' d\rho' \quad (3.4)$$

co2amp supports both Rayleigh-Sommerfeld- Eq. (3.1) and Fresnel- Eq. (3.4) based propagation methods. Also, the user can chose to ignore the **pulse** evolution during free-space propagation.

Eq. (3.1) and Eq. (3.4) assume a monochromatic light, which is not the case for ultrashort pulses that have non-negligible bandwidth. Therefore, in **co2amp** the propagation is calculated in frequency domain: Eq. (3.1) or Eq. (3.4) are applied to Fourier-transformed field in every node of the frequency calculation grid. After that an inverse Fourier transform is used to return to the time domain.

3.3 Optic type A *Active medium*

Active medium is by far the most complex optics that can be used in a **co2amp** project. The models used for simulating the molecular dynamics and pulse amplification are described in a dedicated Chapter 4.

Configuration file for an optic of type A must include specifications of the gas mixture, pumping, and laser transitions included in the simulations. An example of a configuration file is shown below

```
#####
# AM1.yml from 'examples/ATF 5 TW/ATF 3 final amplifier.co2' project

# Semi-diameter of the limiting aperture, m
semiDia: 45e-3

# Length of active medium, m
L: 0.57

# Gas mixture (bar)
p_CO2: 0.50
p_N2: 0.25
p_He: 7.50
O18: 0.472
C13: 0
T0: 300

# Bands included in calculations
band_reg: true
band_seq: true
band_hot: true

# Pumping
pumping: discharge
# Discharge volume, m^3
Vd: 0.0085
# Inter-electrode distance, m
D: 0.085
# Discharge profile
discharge: |
    0.00E+00 0.00000E+00 5.80000E+05
    1.00E-08 1.97186E+03 5.66356E+05
    2.00E-08 3.81445E+03 5.53030E+05
    3.00E-08 5.53410E+03 5.40019E+05
    4.00E-08 7.13691E+03 5.27312E+05
    ...
#####
```

The composition (including isotopic enrichment of carbon dioxide) and the initial temperature of the active medium are specified under the "#Gas mixture (bar)" comment.

For discharge pumping, the geometry of the discharge and its profile must be given. For optical pumping, the wavelength, the absorption cross-section, and the temporal profile of the pumping pulse must be provided.

Comments in the 'optic A (discharge pumped CO2 amplifier).yaml' and 'optic A (optically pumped CO2 amplifier).yaml' template files provide a detailed information on the format of the configuration file.

3.4 Optic type P *Probe*

Probe is a passive **optic**. It doesn't change the field that fits inside its semi-diameter.

$$E(t, \rho) = E'(t, \rho) \quad (3.5)$$

where $E'(t, \rho)$ and $E(t, \rho)$ is the field before- and after- an **optic** respectively.

However, a *Probe* **optic** can be used as a limiting aperture that has a zero transmittance for $\rho > semiDia$. The only configuration parameter for an **optic** of type P is its semi-diameter. A configuration file for a 25 mm semi-diameter *Probe* is shown below

```
#####
# probe

semiDia: 25e-3
#####
```

3.5 Optic type F *Spatial filter*

Spatial filter applies a specified coordinate-dependent transmittance function to a **pulse**

$$E(t, \rho) = E'(t, \rho) \sqrt{\mathcal{T}(\rho)} \quad (3.6)$$

where $\mathcal{T}(\rho)$ is the transmittance function defined in the configuration file.

Configuration example:

```
#####
# spatial filter

semiDia: 25e-3

filter: SIN
r_min: 10e-3
#####
```

See the 'optic F (spatial filter).yaml' template file for details

3.6 Optic type S *Spectral filter*

Spectral filter applies a specified frequency-dependent transmittance function to a **pulse**

$$\begin{aligned} \hat{E}'(\nu, \rho) &= \mathcal{F}(E'(t, \rho)) \\ \hat{E}(\nu, \rho) &= \hat{E}'(\nu, \rho) \sqrt{\mathcal{T}(\nu)} \\ E(t, \rho) &= \mathcal{F}^{-1}(\hat{E}(\nu, \rho)) \end{aligned} \quad (3.7)$$

where \mathcal{F} and \mathcal{F}^{-1} are the Fourier transform and the inverse Fourier transform respectively, ν is the frequency, and $\mathcal{T}(\nu)$ is the transmittance function defined in the configuration file.

Configuration example:

```
#####
# spectral filter

semiDia: 25e-3

filter: FREEFORM
form: |
    32.0e12 1.0
    32.1e12 0.9
    32.2e12 0.7
    32.3e12 0.5
    32.4e12 0.3
    32.5e12 0.0
    32.6e12 0.3
    32.7e12 0.5
    32.8e12 0.7
    32.9e12 0.9
    33.0e12 1.0
#####
```

See the 'optic S (spectral filter).yaml' template file for details

3.7 Optic type L *Lens*

Lens is a lens.

$$\begin{aligned}\hat{E}'(\nu, \rho) &= \mathcal{F}(E'(t, \rho)) \\ \hat{E}(\nu, \rho) &= \hat{E}'(\nu, \rho) \exp\left(-\frac{ik\rho^2}{2F}\right) \\ E(t, \rho) &= \mathcal{F}^{-1}(\hat{E}(\nu, \rho))\end{aligned}\tag{3.8}$$

where $k = \frac{2\pi\nu}{c}$ is the wave number (c is the speed of light) and F is the focal length of the lens.

The calculation is done in frequency domain to ensure that effective focal length is same for all frequencies in the pulse spectrum.

Configuration example (1-meter focal length lens):

```
#####
# lens (F = 1 m)

semiDia: 25e-3

F: 1.0
#####
```

3.8 Optic type M *Material*

In the case of an oblique incidence, effective intensity I_{eff} is reduced and propagation distance in the material (effective thickness) Θ_{eff} is increased automatically depending on the incidence angle θ_i and the refractive

index n of the material

$$\begin{aligned}\theta_r &= \arcsin\left(\frac{\sin\theta_i}{n_0}\right) \\ I_{eff} &= I \frac{\cos\theta_i}{\cos\theta_r} \\ \Theta_{eff} &= \frac{\Theta}{\cos\theta_r}\end{aligned}\tag{3.9}$$

where I and Θ are the intensity before the optic and the actual thickness of the material and θ_r is the refraction angle.

Linear dispersion

$$\begin{aligned}\hat{E}'(\nu, \rho) &= \mathcal{F}(E'(t, \rho)) \\ \hat{E}(\nu, \rho) &= \hat{E}'(\nu, \rho) \exp(2\pi i \Delta\nu) \\ E(t, \rho) &= \mathcal{F}^{-1}(\hat{E}(\nu, \rho))\end{aligned}\tag{3.10}$$

where

$$\Delta\nu = \int_0^\nu (\nu' - \nu_c) \frac{dt}{d\nu'} d\nu' \tag{3.11}$$

c is the speed of light

$$\frac{dt}{d\nu'} = \frac{\Theta_{eff}}{c} \frac{dn_g}{d\nu'} \tag{3.12}$$

ν_c is the central frequency.

where $\hat{E}(\nu, \rho)$ is the field in the frequency domain, \mathcal{F} and \mathcal{F}^{-1} are the Fourier-transform and inverse-Fourier-transform functions, ν is the frequency, ν_c is the central frequency, n_g is the group index of refraction, and Θ is the thickness of the window. The dispersion formulas used for calculating n_0 are given in Appendix C.

Nonlinear interaction

$$\begin{aligned}E(t, \rho) &= E'(t, \rho) \exp\left(2\pi i \nu_c \frac{\Theta_{eff}}{c} n_2 I_{eff}(t, \rho)\right) \\ I_{eff}(t, \rho) &= 2h\nu_c (E'(t, \rho))^2 \frac{\cos\theta_i}{\cos\theta_r}\end{aligned}\tag{3.13}$$

where n_2 is the nonlinear refractive index, h the Plank's constant, and $I(t, r)$ is the field intensity. The numerical values of n_2 used in the program are given in Appendix C.

Configuration example:

```
#=====
# material

semiDia: 25e-3

material: NaCl
thickness: 100e-3
tilt: 0
slices: 10
#=====
```

The following materials are currently supported: CdTe, GaAs, Ge, KCl, NaCl, Si, ZnSe, and air. An arbitrary n_2 can be specified in the configuration file. A pre-defined value (Appendix C) is used otherwise. To improve accuracy, the *Material optic* can be split in several layers. A split-step method is used to calculate linear- and non-linear interaction with a layer: first, a non-linear interaction with a half-layer is calculated, then a full-layer linear interaction, and finally a half-layer nonlinear interaction again.

3.9 Optic type C *Chirper*

Chirper introduces a chirp to a pulse and is typically used to model a stretcher or compressor.

$$\begin{aligned}\widehat{E}'(\nu, \rho) &= \mathcal{F}(E'(t, \rho)) \\ \widehat{E}(\nu, \rho) &= \widehat{E}'(\nu, \rho) \exp(2\pi i \Delta\nu) \\ E(t, \rho) &= \mathcal{F}^{-1}(\widehat{E}(\nu, \rho))\end{aligned}\tag{3.14}$$

where

$$\Delta\nu = \int_0^\nu (\nu' - \nu_c) \frac{dt}{d\nu'} d\nu',\tag{3.15}$$

ν_c is the central frequency, and $\frac{d\nu}{dt}$ is chirpyness.

In the case of linear chirp the chirpyness is constant and and Eq. (3.15) becomes

$$\begin{aligned}\Delta\nu &= \int_0^\nu \frac{\nu' - \nu_c}{\mathcal{C}} d\nu' = \frac{(\nu - \nu_c)^2}{2\mathcal{C}} \\ \mathcal{C} &= \frac{d\nu}{dt}\end{aligned}\tag{3.16}$$

Configuration example:

```
#####
# stretcher (positive chirpyness => red chirp)

semiDia: 25e-3

chirp: LINEAR
c: 3.5e21
#####
```

Only linear chirp is presently supported.

Chapter 4

Modelling of processes in CO₂ amplifiers

4.1 Molecular dynamics

Simulations of active medium pumping by electric discharge and vibrational relaxation are done following Karlov and Konev [4].

4.1.1 Pumping by electric discharge

Pumping is described by the Boltzmann equation in the following form [5, 6]:

$$\begin{aligned} -\frac{1}{3} \left(\frac{\mathcal{E}}{\mathcal{N}} \right)^2 \frac{d}{du} \left[u \left(\sum_j y_j Q_{mj}(u) \right)^{-1} \frac{df(u)}{du} \right] = \\ 1.09 \times 10^{-3} \frac{d}{du} \left[u^2 f(u) \sum_j \frac{y_j}{M_j} Q_{mj}(u) \right] + \sum_{j=1,2} y_j C_j \frac{d}{du} (u f(u)) + 6B y_2 \frac{d}{du} (u Q(u) f) \\ + \sum_j y_j \sum_k (u + u_{jk}) Q_{jk}(u + u_{jk}) f(u + u_{jk}) - u f(u) \sum_j y_j \sum_k Q_{jk}(u) \end{aligned} \quad (4.1)$$

where the left part describes the energy of electrons in the electric field, the first component of the sum of the right part represents energy transfer via elastic collisions between electrons and molecules, the second and third components describe collisions with molecular rotation excitation, and the two last components relate to inelastic collisions with transfer of the energy u_{jk} into vibrational and electronic excitations and ionization.

Electron energy u is expressed in eV;

Ratio of the electric field to the full molecular density, \mathcal{E}/\mathcal{N} , is expressed in units of 10^{-16} V·cm²;

y_j are the relative molecule concentrations ($j = 1$ corresponds to CO₂, $j = 2$ to N₂ and $j = 3$ to He);

$M_1 = 44$, $M_2 = 28$, $M_3 = 4$ are the molar masses;

$C_1 = 8.2 \times 10^{-4}$ eV·Å² [7];

$C_2 = 5.06 \times 10^{-4}$ eV·Å² [8];

$B = 2.5 \times 10^{-4}$ eV is the N₂ rotational constant.

Numerical values of the cross-sections Q and the transferred energies u_{jk} are summarized in Appendix A

Equation 4.1 is solved numerically using the tridiagonal matrix algorithm. Distribution function $f(u)$ is then used in the following calculations.

The rate constant ω_{jk} , and the electron drift speeds v_d are defined as:

$$\omega_{jk} \left[\frac{\text{cm}^3}{\text{s}} \right] = 5.93 \times 10^{-9} \int_0^\infty u Q_{jk}(u) f(u) du \quad (4.2)$$

$$v_d \left[\frac{\text{cm}}{\text{s}} \right] = -5.93 \times 10^7 \left(\frac{1}{3} \frac{\mathcal{E}}{\mathcal{N}} \right) \frac{df(u)}{du} \int_0^\infty u \left(\sum_j y_j Q_{mj}(u) \right)^{-1} du \quad (4.3)$$

The fraction of electron energy transmitted via inelastic processes is defined as

$$z_{jk} = 10^{16} \frac{y_j u_{jk} \omega_{jk}}{\left(\frac{\mathcal{E}}{\mathcal{N}} \right) v_d} \quad (4.4)$$

The fraction of electron energy transmitted to translations and rotations are the following:

$$z_t = 5.93 \times 10^7 \frac{1.09 \times 10^{-3} \int_0^\infty u^2 \left(\sum_j \frac{y_j}{M_j} Q_{mj}(u) \right) f(u) du}{\left(\frac{\mathcal{E}}{\mathcal{N}} \right) v_d} \quad (4.5)$$

$$z_r = 5.93 \times 10^7 \frac{\sum_{j=1,2} y_j C_j \int_0^\infty u f(u) du + 6 y_2 B \int_0^\infty u Q(u) f(u) du}{\left(\frac{\mathcal{E}}{\mathcal{N}} \right) v_d} \quad (4.6)$$

Finally, the distribution of the excitation energy is calculated using the following expressions:

$$\begin{aligned} q_2 &= \sum_{k=1}^6 z_{1k} - \text{fraction of energy transferred to CO}_2 \text{ symmetric stretch } (\nu_1) \text{ and bending } (\nu_2) \text{ modes;} \\ q_3 &= z_{17} - \text{fraction of energy transferred to CO}_2 \text{ asymmetric stretch mode } (\nu_3); \\ q_4 &= \sum_{k=1}^8 z_{2k} - \text{fraction of energy transferred to N}_2 \text{ vibrations;} \\ q_T &= z_t + z_r - \text{fraction of energy transferred to translation and rotation;} \\ q_{ei} &= \sum_{k=9}^{15} z_{2k} + \sum_{k=8}^{10} z_{1k} - \text{fraction of energy spent on excitation of electronic levels and ionization.} \end{aligned}$$

4.1.2 Pumping and vibrational relaxation dynamics

A 3-temperature model is used for describing the vibrational dynamics of the active medium of CO₂ amplifiers. In this model, the following temperatures are used to describe the distribution of the energy between molecular vibrations:

- T_2 – vibrational temperature of ν_1 and ν_2 vibrations of CO₂;
- T_3 – vibrational temperature of the ν_3 vibration of CO₂;
- T_4 – vibrational temperature of N₂.

Vibrational temperatures are related to the average numbers of quanta e_x in the corresponding vibrations as follows:

$$\begin{aligned} e_2 &= \frac{2}{\exp(960/T_2) - 1} \\ e_3 &= \frac{1}{\exp(3380/T_3) - 1} \\ e_4 &= \frac{1}{\exp(3350/T_4) - 1} \end{aligned} \quad (4.7)$$

”2” in the first equation is due to 2-fold degeneracy of the energy levels of the bend vibration.

The dynamics of pumping/relaxation is described by the following equations

$$\begin{aligned}\frac{de_4}{dt} &= p_{e4} - r_a(e_4 - e_3) \\ \frac{de_3}{dt} &= p_{e3} + r_c(e_4 - e_3) - r_3 f_3 \\ \frac{de_2}{dt} &= f_2(p_{e2} + 3r_3 f_3 - r_2(e_2 - e_{2T}))\end{aligned}\tag{4.8}$$

where

$$\begin{aligned}p_{e4} &= 0.8 \times 10^{-3} \frac{q_4}{ny_2} W(t); \quad p_{e3} = 0.8 \times 10^{-3} \frac{q_3}{ny_1} W(t); \quad p_{e2} = 2.8 \times 10^{-3} \frac{q_2}{ny_1} W(t); \\ f_2 &= \frac{2(1+e_2)^2}{2+6e_2+3e_2^2}; \quad f_3 = e_3(1+e_2/2)^3 - (1+e_3)(e_2/2)^3 \exp(-500/T); \\ r_a &= kny_1; \quad r_c = kny_2; \quad r_2 = k_2 n; \quad r_3 = k_3 n; \\ k_2 &= \sum_{i=1}^3 y_i k_{2i}; \quad k_3 = \sum_{i=1}^3 y_i k_{3i}; \\ n &= 273 \frac{p[\text{bar}]}{T_0[\text{K}]}; \\ e_{2T} &= \frac{2}{\exp(960/T) - 1}\end{aligned}\tag{4.9}$$

where $W(t)$ is the discharge power density measured in kW/cm^3 , p_e is measured in μs^{-1} , and the constants k are calculated using the following expressions [9, 10]:

$$\begin{aligned}k &= 240/T^{1/2}; \\ k_{31} &= A(t) \exp(4.138 + 7.945x - 631.24x^2 + 2239x^3); \\ k_{32} &= A(t) \exp(-1.863 + 213.3x - 2796.2x^2 + 9001.9x^3); \\ k_{33} &= A(t) \exp(-3.276 + 291.4x - 3831.8x^2 + 12688x^3); \\ k_{21} &= 1.16 \times 10^3 \exp(-59.3x); \\ k_{22} &= 8.55 \times 10^2 \exp(-69x); \\ k_{23} &= 1.3 \times 10^3 \exp(-40.6x)\end{aligned}\tag{4.10}$$

where $x = T^{-1/3}$, $A(t) = (T/273)(1 + e_{2T}/2)^{-3}$, and temperature T is expressed in K.

Finally, the dynamics of the gas temperature is described by the following equation:

$$\frac{dT}{dt} = \frac{y_1}{C_V} (500r_3 f_3 + 960r_2(e_2 - e_{2T})) + 2.7 \frac{W(t)q_T}{nC_V},\tag{4.11}$$

where $C_V = 2.5(y_1 + y_2) + 1.5y_3$.

4.1.3 Optical pumping

Initial support for optical pumping is included in the `co2amp` code. We assume instant excitation (pump pulse is short compared to vibrational relaxation). The fraction of CO_2 molecules excited by the optical pulse is calculated as

$$\Delta e_3 = e_{max} (1 - \exp(-\Phi\sigma))\tag{4.12}$$

where e_{max} is the saturation population number, Φ is the flux of the pumping photons, and σ is the absorption cross-section. In a classic 2-level system $e_{max} = 0.5$ (maximum 50% of the molecules can be

excited). However, we (rather arbitrary at the moment) use $e_{max} = 1$ in order to allow modeling of multi-photon excitation scenarios.

An adjustment then is made to the average number of quanta in the asymmetric stretch vibration:

$$e_3 = e'_3 + \Delta e_3 \quad (4.13)$$

where $e'_3 = \frac{1}{\exp\left(\frac{3350}{T_0}\right) - 1}$ is the value of e_3 before excitation, and T_0 is the initial temperature of the gas.

For optical pumping at $\sim 3 \mu\text{m}$ through a combinational vibration ($10^0 1, 02^0 1$), e_2 also increases as follows:

$$e_2 = e'_2 + 2\Delta e_3 \times \frac{e'_2}{2e'_1 + e'_2} \quad (4.14)$$

where $e'_1 = \frac{1}{\exp\left(\frac{1920}{T_2}\right) - 1}$, $e'_2 = \frac{2}{\exp\left(\frac{960}{T_2}\right) - 1}$, and the last term takes into account the equilibrium energy distribution between the coupled symmetric stretch and bending vibrations. Several iterations are needed to accurately determine e_2 : The first iteration is done for $T_2 = T_0$; a corrected value of T_2 is then calculated using the first of the equations (4.7), and is used in the next iteration for calculating e_2 , and so forth.

For optical pumping, the dynamics of vibrational relaxation is modeled using equations (4.8) with $p_{e2} = p_{e3} = p_{e4} = 0$.

4.2 Amplification

4.2.1 Laser transitions

Fig. 4.1 shows the vibrational levels and laser transitions included in the **co2amp** amplification model (because of the lack of the spectroscopic data, the sequence and hot bands currently are only supported for natural isotopologue of CO_2 (626^1)).

4.2.2 Main equations

Amplification is simulated in the fast time-frame moving with the pulse using the following equations that also take into account rotational relaxation [11, 12]:

$$\begin{aligned} \frac{\partial E}{\partial z} &= - \sum_J \rho_J, \\ \frac{\partial \rho_J}{\partial t} + \left(2\pi i(\nu_c - \nu_{0J}) + \frac{1}{\tau_2} \right) \rho_J &= - \frac{\sigma_J n_J E}{2\tau_2}, \\ \frac{\partial n_J}{\partial t} + \frac{n_J - n_J^0}{\tau_R} &= 4(\rho_J E^* + c.c.), \end{aligned} \quad (4.15)$$

where summation is done over all rotational-vibrational transitions of all CO_2 isotopologues, and

E - complex field envelope,

ρ_J - polarization of the medium,

z - linear coordinate along the direction of beam propagation,

t - time,

n_J - population inversion of the transition (difference of population densities of upper and lower levels),

n_J^0 - equilibrium population inversion of the transition,

ν_c - carrier frequency,

¹A 3-digit notation commonly is used for designating the isotopologues (molecules with different isotopic composition) of carbon dioxide. In this notation 2, 3 and 4 correspondingly stand for ^{12}C , ^{13}C and ^{14}C ; 6, 7 and 8 represent correspondingly ^{16}O , ^{17}O and ^{18}O . 626 denotes a CO_2 molecule with natural isotopic composition: $^{16}\text{O}-^{12}\text{C}-^{16}\text{O}$.

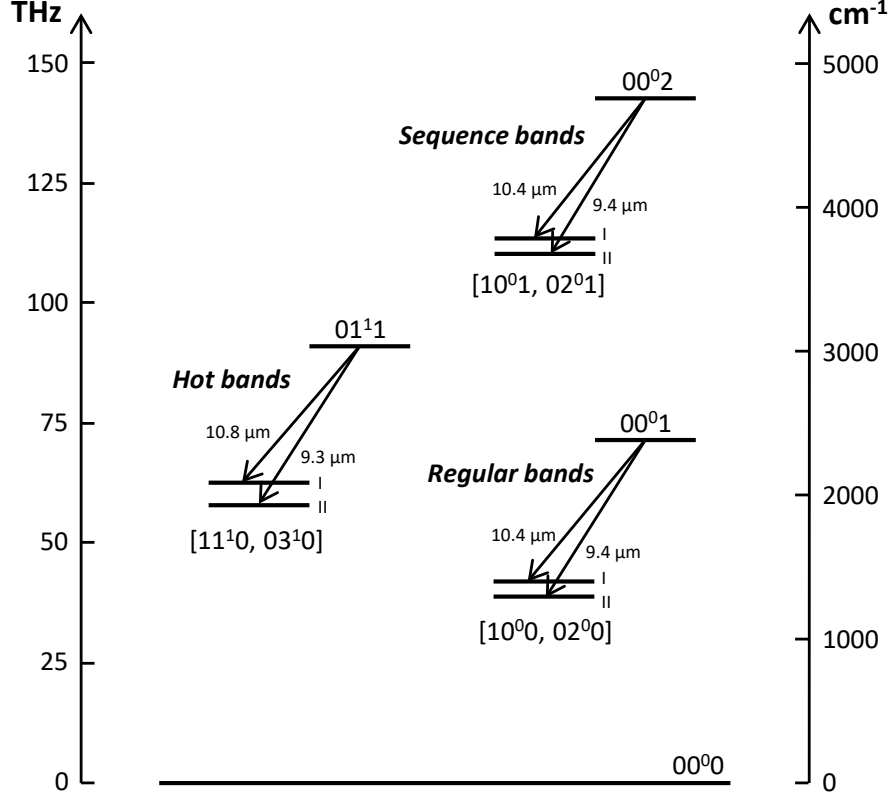


Figure 4.1: Vibrational transitions included in the amplification model. Wavelengths are given for natural CO₂ isotopologue (626).

$\nu_{0,J}$ - transition frequency in the line center,
 σ_J - transition cross-section in the line center,
 τ_2 - polarization dephasing time,
 τ_R - rotational relaxation time.

Transition frequencies of P and R transitions are calculated as follows:

$$\nu_J = \begin{cases} V + B_U(J-1)J - B_L J(J+1) & (P) \\ V + B_U(J+1)(J+2) - B_L J(J+1) & (R) \end{cases} \quad (4.16)$$

where J is the rotational quantum number, V is the vibrational constant of the corresponding transition, and, B_U and B_L the rotational constants of the upper and lower level of the transition correspondingly. The numerical values of the molecular constants used in the program are listed in Appendix B.

The transition cross-section in the line center is calculated [13]

$$\sigma_J[\text{m}^2] = \frac{(\lambda_J[\text{m}])^2 A_J[\text{s}^{-1}]}{4} \times \frac{\tau_2[\text{s}]}{\pi} \quad (4.17)$$

where the first term defines the integral cross-section of the rotational line, and the second term is the maximum of the normalized Lorentzian profile of a line with width $2\pi\Delta\nu_{HWHM} = 1/\tau_2$.

Population inversion in the rotational equilibrium is calculated as

$$n_J^0 = \begin{cases} z(J-1)N_U - z(J)N_L & (P) \\ z(J+1)N_U - z(J)N_L & (R) \end{cases} \quad (4.18)$$

where N_U and N_L are the population densities of the corresponding upper and lower *vibrational* levels, and $z(J)$ is the Boltzmann distribution:

$$z(J) = \begin{cases} 2 \frac{hB}{kT} (2J+1) \exp\left(-\frac{hB}{kT} J(J+1)\right) & (626, 636, 828, 838) \\ \frac{hB}{kT} (2J+1) \exp\left(-\frac{hB}{kT} J(J+1)\right) & (628, 638) \end{cases} \quad (4.19)$$

where $h = 6.62606957 \times 10^{-34}$ J·s and $k = 1.3806488 \times 10^{-23}$ J/K

Optical intensity I is related to the field amplitude as follows:

$$I[\text{W/m}^2] = 2h[\text{J·s}]\nu_c[\text{s}^{-1}]|E|^2 \quad (4.20)$$

Dephasing and relaxation times are defined by the following equations:

$$\begin{aligned} \tau_2[\text{s}] &= \frac{10^{-6}}{\pi \times 7.61 \times 750 \times (P_{CO_2} + 0.733P_{N_2} + 0.64P_{He})} \\ \tau_R[\text{s}] &= \frac{10^{-7}}{750 \times (1.3P_{CO_2} + 1.2P_{N_2} + 0.6P_{He})} \end{aligned} \quad (4.21)$$

where pressure P is measured in bars.

4.2.3 Populations

In the approximation used in the `co2amp` model, the processes of pumping and vibrational relaxation are slow compared to the duration of the pulse. Thus, during the pulse only the stimulated transitions contribute to the change of the populations of the vibrational levels.

In the fast time-frame associated with the pulse there is no equilibrium in the vibrational energy distribution, and a proper population dynamics rather than the temperature model must be used. Thus, during the amplification, population of each rotational-vibrational level is considered independently. After the pulse leaves the active medium, the energy distribution within each vibrational mode becomes normalized quickly, and can be described by the temperature model again.

An important simplification used in the model is the assumption that vibrational temperatures T_2 and T_3 are the same for all CO₂ isotopologues. This assumption can be justified by the relatively small energy mismatch between vibrational levels of different isotopic species of the same molecule, and thus, fast inter-molecular V-V energy exchange. However, this assumption may not hold if the time-delay between two consecutive passes of a pulse through the amplifier is short compared to the relaxation times of intra-mode and inter-isotopic vibrational energy.

Initial populations of vibrational levels are calculated for each isotopologue and for each band using the

following equations:

Regular band

$$N_{00^0 1} = \frac{N}{Q} \exp\left(\frac{-3380}{T_3}\right)$$

$$N_{[10^0 0, 02^0 0]_I} = N_{[10^0 0, 02^0 0]_{II}} = \frac{N}{Q} \exp\left(\frac{-2 \times 960}{T_2}\right)$$

Sequence band

$$N_{00^0 2} = \frac{N}{Q} \exp\left(\frac{-2 \times 3380}{T_3}\right) \quad (4.22)$$

$$N_{[10^0 1, 02^0 1]_I} = N_{[10^0 1, 02^0 1]_{II}} = \frac{N}{Q} \exp\left(\frac{-2 \times 960}{T_2}\right) \exp\left(\frac{-3380}{T_3}\right)$$

Hot band

$$N_{01^1 1} = \frac{N}{Q} \exp\left(\frac{-3380}{T_3}\right) \exp\left(\frac{-960}{T_2}\right)$$

$$N_{[11^1 0, 03^1 0]_I} = N_{[11^1 0, 03^1 0]_{II}} = \frac{N}{Q} \exp\left(\frac{-3 \times 960}{T_2}\right)$$

where N is the density of CO_2 molecules, and Q the partition function [14]:

$$\frac{1}{Q} = \left(1 - \exp\left(\frac{-1920}{T_2}\right)\right) \times \left(1 - \exp\left(\frac{-3380}{T_3}\right)\right) \times \left(1 - \exp\left(\frac{-960}{T_2}\right)\right)^2 \quad (4.23)$$

Change of the populations in the regular band due to stimulated transitions is calculated for each vibrational level using the last of the equations 4.15:

$$\begin{aligned} \frac{d}{dt} N_{00^0 1} &= 2 \sum_{J(00^0 1 \rightarrow [10^0 0, 02^0 0]_{I, II})} (\rho_J E^* + c.c.) \\ \frac{d}{dt} N_{[10^0 0, 02^0 0]_I} &= -2 \sum_{J(00^0 1 \rightarrow [10^0 0, 02^0 0]_I)} (\rho_J E^* + c.c.) \\ \frac{d}{dt} N_{[10^0 0, 02^0 0]_{II}} &= -2 \sum_{J(00^0 1 \rightarrow [10^0 0, 02^0 0]_{II})} (\rho_J E^* + c.c.) \end{aligned} \quad (4.24)$$

where summation is done over all rotational transitions originating or ending at the corresponding vibrational level. Analogous equations are used for the sequence and the hot bands.

Changes of the average quantum numbers in the vibrational modes due to stimulated transitions are calculated as follows:

$$\begin{aligned} \Delta e_3 &= \frac{\Delta N_U}{N}, \\ \Delta e_2 &= -2 \frac{\Delta N_U}{N} \times \frac{e'_2}{2e'_1 + e'_2} \end{aligned} \quad (4.25)$$

wherein the last term in the second equation takes into account the equilibrium energy distribution between the coupled symmetric stretch and bending vibrations, $e'_1 = \frac{1}{\exp\left(\frac{1920}{T_2}\right) - 1}$, $e'_2 = \frac{2}{\exp\left(\frac{960}{T_2}\right) - 1}$, and T_2 is the vibrational temperature before the propagation of the pulse.

New vibrational temperatures then are calculated using the first and second equations 4.7.

Appendices

Appendix A

Cross-sections of excitation processes

Effective cross-sections are expressed in Å; their numerical values in the nodes are given in the tables below (linear interpolation must be used for determining the values in intermediate points); the data and citations are reproduced from [4].

The following notation for cross-sections is used:

Q_{m1} - Transport cross-section of CO₂ [15];

Q_{m2} - Transport cross-section of N₂ [8];

Q_{m3} - Transport cross-section of He [15];

Q - Cross-section of resonant excitation of N₂ rotation [16, 17];

Q_{11} - Cross-section of the process $(000) \rightarrow (01^10)$ [15];

Q_{12} - Cross-section of the process $(000) \rightarrow (100 + 020)$ [15];

$Q_{13}...Q_{16}$ - Cross-sections of resonant processes around 3.8 eV [15];

Q_{17} - Cross-section of the process $(000) \rightarrow (001)$ [15];

$Q_{18}...Q_{1,10}$ - Cross-sections of electronic excitation and ionization of CO₂ [7];

$Q_{21}...Q_{28}$ - Cross-sections of the process $N_2(v=0) \rightarrow N_2(v=1...8)$ [18, 19, 20];

$Q_{29}...Q_{2,15}$ - Cross-sections of electronic excitation and ionization of N₂ [20].

Table A.1: Cross-sections and energies for discharge pumping

| u_i | Q_{m1} | u_i | Q_{m2} | u_i | Q_{m3} | u_i | Q |
|-------|----------|-------|----------|-------|----------|--------|------|
| 0 | 140 | 0 | 1.4 | 0 | 5 | 0.0015 | 0 |
| 0.04 | 84 | 0.001 | 1.4 | 0.01 | 5.4 | 0.05 | 0.1 |
| 0.1 | 55 | 0.002 | 1.6 | 0.1 | 5.8 | 0.25 | 0.65 |
| 0.3 | 21 | 0.008 | 2 | 0.2 | 6.2 | 0.5 | 1.15 |
| 0.5 | 10.8 | 0.01 | 2.2 | 1 | 6.5 | 0.8 | 2 |
| 0.6 | 9.4 | 0.04 | 4 | 2 | 6.1 | 1 | 2.65 |
| 1 | 5.7 | 0.08 | 6 | 7 | 5 | 1.5 | 5.6 |
| 1.7 | 5 | 0.1 | 6.5 | 10 | 4.1 | 1.8 | 7.5 |
| 2 | 5.1 | 0.2 | 8.8 | 20 | 3 | 1.9 | 8.2 |
| 2.5 | 6 | 0.3 | 9.8 | | | 2 | 8.6 |
| 3 | 7.7 | 0.4 | 10 | | | 2.15 | 8.95 |
| 4.1 | 9.4 | 1 | 10 | | | 2.43 | 9 |
| 5 | 14.5 | 1.2 | 11 | | | 2.6 | 8.9 |
| 7.4 | 10 | 1.4 | 12.5 | | | 2.75 | 8.4 |
| 10 | 11.7 | 1.8 | 20 | | | 2.9 | 7.65 |
| 20 | 16 | 2 | 25 | | | 3.25 | 6.2 |
| 27 | 16.3 | 2.5 | 30 | | | 3.6 | 5.1 |
| 50 | 13 | 3 | 26 | | | 4 | 4.5 |
| | | 4 | 15 | | | 4.5 | 4.16 |
| | | 5 | 12 | | | 5 | 3.97 |
| | | 7 | 10 | | | 5.5 | 3.93 |
| | | 10 | 10 | | | 7 | 4.17 |
| | | 14 | 11 | | | 9 | 4.46 |
| | | 18 | 12.2 | | | 11 | 4.42 |
| | | 20 | 12 | | | 15 | 3.94 |
| | | 30 | 10 | | | 22 | 3.15 |
| | | 100 | 10 | | | 25 | 3.05 |

Table A.2: Cross-sections and energies for discharge pumping - continued

| u_i | Q_{11} | u_i | Q_{12} | u_i | Q_{13} | u_i | Q_{14} | u_i | Q_{15} |
|-----------------------------|----------|-----------------------------|----------|-----------------------------|----------|-----------------------------|----------|------------------------------|------------|
| 0.083 | 0 | 0.167 | 0 | 0.252 | 0 | 2.37 | 0 | 2.37 | 0 |
| 0.085 | 0.36 | 0.2 | 0.54 | 2.7 | 0.25 | 3 | 0.26 | 3 | 0.17 |
| 0.09 | 1.04 | 0.25 | 0.82 | 3 | 0.4 | 3.5 | 0.52 | 3.65 | 0.33 |
| 0.1 | 1.6 | 0.3 | 0.82 | 3.3 | 0.6 | 4 | 0.5 | 3.8 | 0.31 |
| 0.12 | 1.84 | 0.5 | 0.68 | 3.6 | 0.65 | 4.5 | 0.22 | 4 | 0.21 |
| 0.14 | 2.12 | 0.7 | 0.56 | 4.5 | 0.23 | 4.6 | 0.1 | 4.3 | 0.1 |
| 0.16 | 2.16 | 1 | 0.47 | 4.6 | 0.1 | 5 | 0 | 5 | 0 |
| 0.2 | 2.08 | 1.4 | 0.45 | 5 | 0 | | | | |
| 0.3 | 1.76 | 2 | 0.55 | | | | | | |
| 0.4 | 1.52 | 3 | 1.15 | | | | | | |
| 0.5 | 1.28 | 3.9 | 1.83 | | | | | | |
| 0.6 | 1.08 | 4.5 | 1.4 | | | | | | |
| 0.8 | 0.8 | 5 | 0.4 | | | | | | |
| 1 | 0.58 | 6 | 0.28 | | | | | | |
| 1.2 | 0.48 | 10 | 0.2 | | | | | | |
| 1.6 | 0.34 | 20 | 0.1 | | | | | | |
| 1.8 | 0.35 | | | | | | | | |
| 2 | 0.4 | | | | | | | | |
| 2.5 | 0.64 | | | | | | | | |
| 3 | 1.04 | | | | | | | | |
| 3.7 | 1.4 | | | | | | | | |
| 4 | 1.36 | | | | | | | | |
| 4.2 | 1.2 | | | | | | | | |
| 4.5 | 0.92 | | | | | | | | |
| 5 | 0.53 | | | | | | | | |
| 6 | 0.4 | | | | | | | | |
| 8 | 0.36 | | | | | | | | |
| 9 | 0.28 | | | | | | | | |
| 10 | 0.16 | | | | | | | | |
| 10.1 | 0 | | | | | | | | |
| $u_{11} = 0.083 \text{ eV}$ | | $u_{12} = 0.167 \text{ eV}$ | | $u_{13} = 0.252 \text{ eV}$ | | $u_{14} = 0.339 \text{ eV}$ | | $u_{15} = 0.422 \text{ eV}$ | |
| u_i | Q_{16} | u_i | Q_{17} | u_i | Q_{18} | u_i | Q_{19} | u_i | $Q_{1,10}$ |
| 2.5 | 0 | 0.29 | 0 | 7 | 0 | 10.5 | 0 | 13.8 | 0 |
| 3 | 0.19 | 0.3 | 0.44 | 8 | 0.5 | 11.5 | 0.56 | 15 | 0.1 |
| 3.6 | 0.245 | 0.35 | 0.65 | 8.4 | 0.6 | 14 | 0.8 | 16 | 0.13 |
| 4 | 0.21 | 0.4 | 0.73 | 9 | 0.46 | 20 | 1.2 | 17 | 0.17 |
| 5.07 | 0 | 0.5 | 0.84 | 10 | 0.175 | 30 | 2 | 30 | 1.55 |
| | | 0.8 | 1 | 10.5 | 0 | 50 | 4 | 40 | 2.1 |
| | | 1 | 1 | | | | | | |
| | | 2 | 0.78 | | | | | | |
| | | 6 | 0.37 | | | | | | |
| | | 10 | 0.25 | | | | | | |
| | | 50 | 0 | | | | | | |
| $u_{16} = 2.5 \text{ eV}$ | | $u_{17} = 0.29 \text{ eV}$ | | $u_{18} = 7 \text{ eV}$ | | $u_{19} = 10.5 \text{ eV}$ | | $u_{1,10} = 13.8 \text{ eV}$ | |

Table A.3: Cross-sections and energies for discharge pumping - continued

| u_i | Q_{21} | u_i | Q_{22} | u_i | Q_{23} | u_i | Q_{24} | u_i | Q_{25} |
|---------------------|------------|-----------------------|------------|----------------------|------------|--------------------|------------|----------------------|------------|
| 0.29 | 0 | 1.83 | 0 | 1.9 | 0 | 2.05 | 0 | 2.1 | 0 |
| 0.5 | 0.0052 | 1.9 | 0.208 | 2 | 0.416 | 2.1 | 0.416 | 2.15 | 0.208 |
| 0.8 | 0.0083 | 2 | 1.46 | 2.1 | 1.33 | 2.2 | 1.16 | 2.2 | 0.541 |
| 1 | 0.0104 | 2.05 | 2.29 | 2.2 | 1.87 | 2.26 | 1.58 | 2.3 | 0.915 |
| 1.2 | 0.0166 | 2.1 | 1.66 | 2.3 | 1.25 | 2.55 | 0 | 2.46 | 1.12 |
| 1.3 | 0.0728 | 2.2 | 0.79 | 2.36 | 0.208 | 2.75 | 0.832 | 2.5 | 1.12 |
| 1.4 | 0.135 | 2.35 | 0.208 | 2.42 | 0 | 2.77 | 0 | 2.6 | 0.208 |
| 1.6 | 0.25 | 2.45 | 1.98 | 2.5 | 0.499 | 3 | 0.208 | 2.62 | 0 |
| 1.8 | 0.52 | 2.5 | 1.78 | 2.61 | 0.915 | 3.05 | 0.208 | 2.68 | 0 |
| 1.9 | 0.832 | 2.62 | 0.208 | 2.7 | 0.624 | 3.25 | 0 | 2.8 | 0.416 |
| 2 | 3.02 | 2.75 | 1.04 | 2.75 | 0.208 | | | 2.9 | 0.75 |
| 2.05 | 3.12 | 2.95 | 1.66 | 2.8 | 0 | | | 3 | 0 |
| 2.1 | 2.08 | 3.05 | 0.624 | 2.92 | 0.416 | | | 3.2 | 0.25 |
| 2.15 | 1.25 | 3.2 | 0.208 | 3 | 0.208 | | | 3.3 | 0.125 |
| 2.2 | 0.832 | 3.4 | 0.208 | 3.25 | 0.208 | | | 3.35 | 0 |
| 2.3 | 2.9 | 4 | 0 | 3.31 | 0 | | | | |
| 2.45 | 1.04 | | | | | | | | |
| 2.53 | 1.25 | | | | | | | | |
| 2.6 | 1.75 | | | | | | | | |
| 2.62 | 2.08 | | | | | | | | |
| 2.68 | 1.73 | | | | | | | | |
| 2.73 | 0.416 | | | | | | | | |
| 2.85 | 0.32 | | | | | | | | |
| 2.92 | 0.416 | | | | | | | | |
| 3.12 | 0.728 | | | | | | | | |
| 3.3 | 0.52 | | | | | | | | |
| 4 | 0 | | | | | | | | |
| $u_{21} = 0.29$ eV | | $u_{22} = 0.58$ eV | | $u_{23} = 0.87$ eV | | $u_{24} = 1.16$ eV | | $u_{25} = 1.45$ eV | |
| u_i | Q_{26} | u_i | Q_{27} | u_i | Q_{28} | u_i | Q_{29} | u_i | $Q_{2,10}$ |
| 2.3 | 0 | 2.4 | 0 | 2.6 | 0 | 5 | 0 | 6.8 | 0 |
| 2.4 | 0.75 | 2.5 | 0.208 | 2.7 | 0.208 | 5.9 | 0.41 | 7.1 | 0.57 |
| 2.5 | 1.04 | 2.75 | 0.75 | 2.9 | 0.29 | 6.1 | 0.41 | 8.1 | 0.57 |
| 2.55 | 1.12 | 3 | 0 | 3 | 0.208 | 7 | 0.07 | 8.6 | 0.25 |
| 2.6 | 1.04 | 3.2 | 0.166 | 3.1 | 0 | 9 | 0 | 9.5 | 0.12 |
| 2.65 | 0.624 | 3.3 | 0.146 | 3.2 | 0 | | | 20.7 | 0 |
| 2.7 | 0.416 | 3.4 | 0 | 3.3 | 1.04 | | | | |
| 2.8 | 0.208 | | | 3.4 | 0 | | | | |
| 2.9 | 0.125 | | | | | | | | |
| 3 | 2.5 | | | | | | | | |
| 3.1 | 0.166 | | | | | | | | |
| 3.2 | 0 | | | | | | | | |
| $u_{26} = 1.74$ eV | | $u_{27} = 2.03$ eV | | $u_{28} = 2.32$ eV | | $u_{29} = 5$ eV | | $u_{2,10} = 6.8$ eV | |
| u_i | $Q_{2,11}$ | u_i | $Q_{2,12}$ | u_i | $Q_{2,13}$ | u_i | $Q_{2,14}$ | u_i | $Q_{2,15}$ |
| 8.4 | 0 | 11.25 | 0 | 12.5 | 0 | 14 | 0 | 15.6 | 0 |
| 8.7 | 0.42 | 13.8 | 0.41 | 13 | 0.4 | 14.3 | 1.7 | 18 | 0.1 |
| 9.1 | 0.42 | 14 | 1 | 13.6 | 0.4 | 14.8 | 1.7 | 20 | 0.21 |
| 10 | 0.3 | 14.7 | 1 | 14 | 0.16 | 15.6 | 0.2 | 50 | 2.52 |
| 20.7 | 0 | 15 | 0.25 | 20.7 | 0 | 20.6 | 0.2 | 100 | 2.52 |
| | | 65 | 0 | | | 25.4 | 2.8 | | |
| | | | | | | 100 | 2.8 | | |
| $u_{2,11} = 8.4$ eV | | $u_{2,12} = 11.25$ eV | | $u_{2,13} = 12.5$ eV | | $u_{2,14} = 14$ eV | | $u_{2,15} = 15.6$ eV | |

Appendix B

Molecular constants

The vibrational and rotational constants V and B are listed in Table B.1.

Einstein coefficients A of the laser transitions included in the simulations are summarized in Tables B.2-B.7. Except for the sequence band of 828 isotopologue and the 10-micron transitions of 838 isotopologue, data are taken from the HITRAN2016 database [21] (Einstein coefficients) and our fit of HITRAN data with equation (4.16) (V and B).

For the sequence band of 828 (not included in the HITRAN database), V constants are roughly estimated assuming same shift from 628 as in the regular band, and B constants are assumed to be $\sim 1\%$ lower than that of regular and hot bands, in analogy with other isotopologues. Einstein coefficients are assumed $\sim 2\times$ larger than those of the regular band in analogy with other isotopologues.

For the 10-micron transitions of 838 (not included in the HITRAN database), V and B constants are taken from [22]. Einstein coefficients are obtained by scaling the coefficients of the corresponding 9-micron transitions in the assumption that gain coefficients (proportional to transition cross-sections, Eq. 4.17) are roughly the same (according to Freed's measurements [23]).

Table B.1: Molecular constants of CO₂ isotopologues, THz

| | 626 | 628 | 828 | 636 | 638 | 838 |
|--|----------|----------|----------|----------|----------|----------|
| 00 ⁰ 1 → [10 ⁰ 0, 02 ⁰ 0] _{I,II} ('Regular band') | | | | | | |
| $V(00^0_1 - I)$ | 28.809 | 28.969 | 28.988 | 27.384 | 27.692 | 27.839 |
| $V(00^0_1 - II)$ | 31.889 | 32.158 | 32.489 | 30.508 | 30.610 | 30.786 |
| $B(00^0_1)$ | 0.011589 | 0.010936 | 0.010303 | 0.011593 | 0.010939 | 0.010315 |
| $B([10^0_0, 02^0_0]_I)$ | 0.011683 | 0.011034 | 0.010403 | 0.011668 | 0.011019 | 0.010403 |
| $B([10^0_0, 02^0_0]_{II})$ | 0.011687 | 0.011019 | 0.010375 | 0.011700 | 0.011031 | 0.010394 |
| 00 ⁰ 2 → [10 ⁰ 1, 02 ⁰ 1] _{I,II} ('Sequence band') | | | | | | |
| $V(00^0_2 - I)$ | 28.737 | 28.911 | [28.93] | 27.300 | - | - |
| $V(00^0_2 - II)$ | 31.792 | 32.029 | [32.36] | 30.453 | - | - |
| $B(00^0_2)$ | 0.011497 | 0.010859 | [0.0103] | 0.011512 | - | - |
| $B([10^0_1, 02^0_1]_I)$ | 0.011588 | 0.010955 | [0.0103] | 0.011585 | - | - |
| $B([10^0_1, 02^0_1]_{II})$ | 0.011598 | 0.010946 | [0.0103] | 0.011623 | - | - |
| 01 ^{1e} 1 → [11 ^{1e} 0, 03 ^{1e} 0] _{I,II} ('Hot-e band') | | | | | | |
| $V(01^{1e}_1 - I)$ | 27.796 | 27.964 | 20.190 | 26.476 | 26.749 | - |
| $V(01^{1e}_1 - II)$ | 32.124 | 32.388 | 32.690 | 30.689 | 30.832 | - |
| $B(01^{1e}_1)$ | 0.011602 | 0.010949 | 0.010324 | 0.011605 | 0.010953 | - |
| $B([11^{1e}0, 03^{1e}0]_I)$ | 0.011687 | 0.011036 | 0.010412 | 0.011676 | 0.011028 | - |
| $B([11^{1e}0, 03^{1e}0]_{II})$ | 0.011695 | 0.011032 | 0.010398 | 0.011702 | 0.011040 | - |
| 01 ^{1f} 1 → [11 ^{1f} 0, 03 ^{1f} 0] _{I,II} ('Hot-f band') | | | | | | |
| $V(01^{1f}_1 - I)$ | 27.796 | 27.964 | 28.019 | 26.476 | 26.749 | - |
| $V(01^{1f}_1 - II)$ | 32.124 | 32.388 | 32.690 | 30.689 | 30.832 | - |
| $B(01^{1f}_1)$ | 0.011620 | 0.010965 | 0.010338 | 0.011623 | 0.010970 | - |
| $B([11^{1f}0, 03^{1f}0]_I)$ | 0.011716 | 0.011063 | 0.010437 | 0.011703 | 0.011053 | - |
| $B([11^{1f}0, 03^{1f}0]_{II})$ | 0.011723 | 0.011055 | 0.010417 | 0.011733 | 0.011066 | - |

Table B.2: Einstein coefficients A of laser transitions of '626' CO₂, s⁻¹

| J | Regular | | | Sequence | | | Hot-e | | | Hot-f | | |
|-----|---------|-------|-------|----------|-------|-------|-------|-------|-------|-------|-------|-------|
| | 10P | 10R | 9P | 9R | 10P | 10R | 9P | 9R | 10P | 10R | 9P | 9R |
| 0 | - | 0.130 | - | 0.145 | - | - | - | - | - | - | - | - |
| 1 | - | - | - | - | 0.809 | 0.324 | 0.800 | 0.322 | - | - | - | - |
| 2 | 0.260 | 0.168 | 0.289 | 0.187 | - | - | - | - | 0.176 | 0.135 | 0.216 | 0.166 |
| 3 | - | - | - | - | 0.484 | 0.361 | 0.478 | 0.359 | 0.188 | 0.147 | 0.230 | 0.182 |
| 4 | 0.222 | 0.178 | 0.247 | 0.199 | - | - | - | - | 0.188 | 0.155 | 0.231 | 0.191 |
| 5 | - | - | - | - | 0.447 | 0.376 | 0.442 | 0.374 | 0.188 | 0.159 | 0.229 | 0.197 |
| 6 | 0.212 | 0.184 | 0.235 | 0.205 | - | - | - | - | 0.185 | 0.164 | 0.226 | 0.204 |
| 7 | - | - | - | - | 0.432 | 0.384 | 0.427 | 0.383 | 0.185 | 0.167 | 0.223 | 0.208 |
| 8 | 0.206 | 0.186 | 0.229 | 0.209 | 0.423 | 0.389 | 0.418 | 0.389 | 0.183 | 0.166 | 0.225 | 0.206 |
| 9 | - | - | - | - | - | - | - | - | 0.182 | 0.169 | 0.222 | 0.210 |
| 10 | 0.203 | 0.188 | 0.225 | 0.212 | 0.417 | 0.392 | 0.413 | 0.394 | 0.180 | 0.170 | 0.219 | 0.214 |
| 11 | - | - | - | - | - | - | - | - | 0.179 | 0.172 | 0.219 | 0.215 |
| 12 | 0.200 | 0.190 | 0.223 | 0.215 | 0.412 | 0.395 | 0.409 | 0.398 | 0.177 | 0.173 | 0.215 | 0.220 |
| 13 | - | - | - | - | 0.408 | 0.396 | 0.406 | 0.401 | 0.176 | 0.174 | 0.214 | 0.223 |
| 14 | 0.198 | 0.191 | 0.221 | 0.217 | - | - | - | - | 0.171 | 0.171 | 0.216 | 0.218 |
| 15 | - | - | - | - | 0.405 | 0.398 | 0.403 | 0.405 | 0.175 | 0.172 | 0.213 | 0.223 |
| 16 | 0.196 | 0.192 | 0.219 | 0.218 | 0.402 | 0.399 | 0.401 | 0.408 | 0.175 | 0.172 | 0.212 | 0.224 |
| 17 | - | - | - | - | 0.399 | 0.399 | 0.400 | 0.411 | 0.174 | 0.172 | 0.211 | 0.226 |
| 18 | 0.195 | 0.192 | 0.218 | 0.220 | - | - | - | - | 0.173 | 0.172 | 0.210 | 0.227 |
| 19 | - | - | - | - | 0.387 | 0.400 | 0.395 | 0.423 | 0.172 | 0.172 | 0.209 | 0.229 |
| 20 | 0.193 | 0.192 | 0.217 | 0.222 | 0.384 | 0.399 | 0.394 | 0.425 | 0.171 | 0.171 | 0.208 | 0.230 |
| 21 | - | - | - | - | 0.381 | 0.399 | 0.393 | 0.428 | 0.170 | 0.171 | 0.208 | 0.231 |
| 22 | 0.192 | 0.193 | 0.216 | 0.223 | 0.378 | 0.398 | 0.393 | 0.432 | 0.169 | 0.171 | 0.207 | 0.233 |
| 23 | - | - | - | - | 0.375 | 0.397 | 0.392 | 0.435 | 0.168 | 0.170 | 0.207 | 0.234 |
| 24 | 0.190 | 0.193 | 0.215 | 0.225 | 0.372 | 0.396 | 0.392 | 0.438 | 0.167 | 0.170 | 0.206 | 0.236 |
| 25 | - | - | - | - | 0.369 | 0.395 | 0.392 | 0.441 | 0.166 | 0.169 | 0.205 | 0.237 |
| 26 | 0.189 | 0.193 | 0.215 | 0.226 | 0.366 | 0.393 | 0.391 | 0.444 | 0.165 | 0.168 | 0.205 | 0.239 |
| 27 | - | - | - | - | 0.363 | 0.392 | 0.391 | 0.447 | 0.164 | 0.168 | 0.204 | 0.240 |
| 28 | 0.188 | 0.193 | 0.214 | 0.228 | 0.359 | 0.390 | 0.391 | 0.451 | 0.163 | 0.167 | 0.204 | 0.241 |
| 29 | - | - | - | - | 0.356 | 0.388 | 0.391 | 0.454 | 0.162 | 0.166 | 0.203 | 0.243 |
| 30 | 0.186 | 0.192 | 0.214 | 0.229 | 0.352 | 0.387 | 0.391 | 0.458 | 0.161 | 0.165 | 0.203 | 0.244 |
| 31 | - | - | - | - | 0.349 | 0.385 | 0.391 | 0.461 | 0.160 | 0.164 | 0.202 | 0.246 |
| 32 | 0.185 | 0.192 | 0.213 | 0.231 | 0.345 | 0.382 | 0.391 | 0.465 | 0.159 | 0.163 | 0.202 | 0.247 |
| 33 | - | - | - | - | 0.342 | 0.380 | 0.391 | 0.468 | 0.157 | 0.162 | 0.202 | 0.249 |
| 34 | 0.183 | 0.192 | 0.213 | 0.232 | 0.338 | 0.377 | 0.392 | 0.472 | 0.150 | 0.150 | 0.207 | 0.248 |
| 35 | - | - | - | - | - | - | - | - | - | - | - | - |
| 36 | 0.182 | 0.191 | 0.212 | 0.234 | - | - | - | - | - | - | - | - |
| 37 | - | - | - | - | - | - | - | - | - | - | - | - |
| 38 | 0.181 | 0.191 | 0.212 | 0.236 | - | - | - | - | - | - | - | - |
| 39 | - | - | - | - | - | - | - | - | - | - | - | - |
| 40 | 0.179 | 0.190 | 0.212 | 0.237 | - | - | - | - | - | - | - | - |
| 41 | - | - | - | - | - | - | - | - | - | - | - | - |
| 42 | 0.177 | 0.190 | 0.212 | 0.239 | - | - | - | - | - | - | - | - |
| 43 | - | - | - | - | - | - | - | - | - | - | - | - |
| 44 | 0.176 | 0.189 | 0.211 | 0.241 | - | - | - | - | - | - | - | - |
| 45 | - | - | - | - | - | - | - | - | - | - | - | - |
| 46 | 0.174 | 0.188 | 0.211 | 0.242 | - | - | - | - | - | - | - | - |
| 47 | - | - | - | - | - | - | - | - | - | - | - | - |
| 48 | 0.173 | 0.187 | 0.211 | 0.244 | - | - | - | - | - | - | - | - |
| 49 | - | - | - | - | - | - | - | - | - | - | - | - |
| 50 | 0.171 | 0.186 | 0.211 | 0.246 | - | - | - | - | - | - | - | - |
| 51 | - | - | - | - | - | - | - | - | - | - | - | - |
| 52 | 0.169 | 0.185 | 0.211 | 0.248 | - | - | - | - | - | - | - | - |
| 53 | - | - | - | - | - | - | - | - | - | - | - | - |
| 54 | 0.167 | 0.184 | 0.211 | 0.249 | - | - | - | - | - | - | - | - |
| 55 | - | - | - | - | - | - | - | - | - | - | - | - |
| 56 | 0.166 | 0.183 | 0.211 | 0.251 | - | - | - | - | - | - | - | - |
| 57 | - | - | - | - | - | - | - | - | - | - | - | - |
| 58 | 0.164 | 0.182 | 0.211 | 0.253 | - | - | - | - | - | - | - | - |
| 59 | - | - | - | - | - | - | - | - | - | - | - | - |
| 60 | 0.162 | - | 0.211 | - | - | - | - | - | - | - | - | - |

Table B.3: Einstein coefficients A of laser transitions of $'628'$ CO₂, s⁻¹

| J | Regular | | | Sequence | | | Hot-e | | | Hot-f | | |
|-----|---------|-------|-------|----------|-------|-------|-------|-------|-------|-------|-------|-------|
| | 10P | 10R | 9P | 10P | 10R | 9P | 10P | 10R | 9P | 10P | 10R | 9P |
| 0 | - | 0.100 | - | - | - | - | - | - | - | - | - | - |
| 1 | 0.298 | 0.120 | 0.574 | - | - | - | 0.162 | 0.089 | - | 0.162 | 0.089 | - |
| 2 | 0.199 | 0.128 | 0.382 | - | - | - | 0.206 | 0.148 | 0.268 | 0.206 | 0.148 | 0.268 |
| 3 | 0.179 | 0.133 | 0.343 | - | - | - | 0.225 | 0.157 | 0.285 | 0.225 | 0.157 | 0.285 |
| 4 | 0.170 | 0.136 | 0.326 | - | 0.287 | 0.611 | 0.493 | 0.158 | 0.286 | 0.493 | 0.158 | 0.286 |
| 5 | 0.165 | 0.139 | 0.317 | 0.348 | 0.292 | 0.593 | 0.501 | 0.157 | 0.284 | 0.501 | 0.157 | 0.284 |
| 6 | 0.162 | 0.140 | 0.311 | 0.341 | 0.295 | 0.581 | 0.508 | 0.156 | 0.282 | 0.508 | 0.156 | 0.282 |
| 7 | 0.159 | 0.141 | 0.306 | 0.336 | 0.298 | 0.573 | 0.513 | 0.155 | 0.280 | 0.513 | 0.155 | 0.280 |
| 8 | 0.158 | 0.142 | 0.303 | 0.332 | 0.300 | 0.567 | 0.517 | 0.154 | 0.278 | 0.517 | 0.154 | 0.278 |
| 9 | 0.156 | 0.143 | 0.300 | 0.329 | 0.302 | 0.562 | 0.521 | 0.154 | 0.277 | 0.521 | 0.154 | 0.277 |
| 10 | 0.155 | 0.144 | 0.298 | 0.327 | 0.303 | 0.558 | 0.524 | 0.153 | 0.275 | 0.524 | 0.153 | 0.275 |
| 11 | 0.154 | 0.144 | 0.296 | 0.324 | 0.304 | 0.555 | 0.527 | 0.152 | 0.274 | 0.527 | 0.152 | 0.274 |
| 12 | 0.153 | 0.145 | 0.295 | 0.323 | 0.305 | 0.552 | 0.530 | 0.152 | 0.273 | 0.530 | 0.152 | 0.273 |
| 13 | 0.152 | 0.145 | 0.294 | 0.321 | 0.306 | 0.549 | 0.532 | 0.151 | 0.272 | 0.532 | 0.151 | 0.272 |
| 14 | 0.152 | 0.145 | 0.292 | 0.319 | 0.307 | 0.547 | 0.534 | 0.151 | 0.271 | 0.534 | 0.151 | 0.271 |
| 15 | 0.151 | 0.146 | 0.291 | 0.318 | 0.307 | 0.545 | 0.537 | 0.150 | 0.270 | 0.537 | 0.150 | 0.270 |
| 16 | 0.150 | 0.146 | 0.290 | 0.316 | 0.308 | 0.543 | 0.538 | 0.150 | 0.269 | 0.538 | 0.149 | 0.270 |
| 17 | 0.150 | 0.146 | 0.289 | 0.315 | 0.308 | 0.542 | 0.541 | 0.149 | 0.268 | 0.541 | 0.148 | 0.269 |
| 18 | 0.149 | 0.146 | 0.289 | 0.314 | 0.309 | 0.540 | 0.542 | 0.149 | 0.268 | 0.542 | 0.148 | 0.269 |
| 19 | 0.148 | 0.146 | 0.288 | 0.312 | 0.309 | 0.539 | 0.544 | 0.148 | 0.267 | 0.544 | 0.147 | 0.268 |
| 20 | 0.148 | 0.146 | 0.287 | 0.311 | 0.309 | 0.538 | 0.546 | 0.148 | 0.266 | 0.546 | 0.147 | 0.267 |
| 21 | 0.147 | 0.147 | 0.287 | 0.310 | 0.309 | 0.537 | 0.548 | 0.148 | 0.266 | 0.548 | 0.146 | 0.267 |
| 22 | 0.147 | 0.147 | 0.286 | 0.309 | 0.309 | 0.535 | 0.550 | 0.147 | 0.265 | 0.550 | 0.146 | 0.266 |
| 23 | 0.146 | 0.147 | 0.285 | 0.308 | 0.309 | 0.534 | 0.551 | 0.147 | 0.264 | 0.551 | 0.145 | 0.266 |
| 24 | 0.146 | 0.147 | 0.285 | 0.307 | 0.309 | 0.533 | 0.553 | 0.147 | 0.264 | 0.553 | 0.145 | 0.265 |
| 25 | 0.145 | 0.146 | 0.284 | 0.305 | 0.309 | 0.532 | 0.555 | 0.146 | 0.263 | 0.555 | 0.144 | 0.265 |
| 26 | 0.144 | 0.146 | 0.284 | 0.304 | 0.309 | 0.532 | 0.556 | 0.146 | 0.262 | 0.556 | 0.144 | 0.264 |
| 27 | 0.144 | 0.146 | 0.283 | 0.303 | 0.309 | 0.531 | 0.558 | 0.145 | 0.262 | 0.558 | 0.143 | 0.264 |
| 28 | 0.143 | 0.146 | 0.283 | 0.302 | 0.309 | 0.530 | 0.559 | 0.145 | 0.262 | 0.559 | 0.143 | 0.263 |
| 29 | 0.143 | 0.146 | 0.282 | 0.301 | 0.309 | 0.529 | 0.561 | 0.145 | 0.261 | 0.561 | 0.142 | 0.263 |
| 30 | 0.142 | 0.146 | 0.282 | 0.300 | 0.308 | 0.528 | 0.563 | 0.144 | 0.261 | 0.563 | 0.142 | 0.263 |
| 31 | 0.142 | 0.146 | 0.282 | 0.301 | 0.308 | 0.528 | 0.564 | 0.144 | 0.260 | 0.564 | 0.141 | 0.262 |
| 32 | 0.141 | 0.146 | 0.281 | 0.297 | 0.308 | 0.527 | 0.566 | 0.144 | 0.260 | 0.566 | 0.141 | 0.262 |
| 33 | 0.141 | 0.146 | 0.281 | - | - | 0.526 | 0.568 | 0.143 | 0.259 | 0.568 | 0.141 | 0.261 |
| 34 | 0.140 | 0.145 | 0.280 | - | - | 0.526 | 0.569 | 0.143 | 0.259 | 0.569 | 0.140 | 0.261 |
| 35 | 0.139 | 0.145 | 0.280 | - | - | 0.525 | 0.570 | 0.142 | 0.259 | 0.570 | 0.139 | 0.261 |
| 36 | 0.139 | 0.145 | 0.280 | - | - | 0.525 | 0.572 | 0.142 | 0.258 | 0.572 | 0.139 | 0.261 |
| 37 | 0.138 | 0.145 | 0.279 | - | - | 0.524 | 0.574 | 0.142 | 0.258 | 0.574 | 0.138 | 0.260 |
| 38 | 0.138 | 0.144 | 0.279 | - | - | 0.523 | 0.575 | 0.141 | 0.257 | 0.575 | 0.138 | 0.260 |
| 39 | 0.137 | 0.144 | 0.279 | - | - | 0.523 | 0.577 | 0.141 | 0.257 | 0.577 | 0.137 | 0.260 |
| 40 | 0.136 | 0.144 | 0.279 | - | - | 0.522 | 0.579 | 0.140 | 0.256 | 0.579 | 0.137 | 0.259 |
| 41 | 0.136 | 0.143 | 0.278 | - | - | - | - | 0.140 | 0.256 | - | 0.137 | 0.259 |
| 42 | 0.135 | 0.143 | 0.278 | - | - | - | - | 0.139 | 0.256 | - | 0.136 | 0.258 |
| 43 | 0.134 | 0.143 | 0.278 | - | - | - | - | 0.139 | 0.255 | - | 0.135 | 0.258 |
| 44 | 0.134 | 0.142 | 0.277 | - | - | - | - | 0.139 | 0.255 | - | 0.135 | 0.258 |
| 45 | 0.133 | 0.142 | 0.277 | - | - | - | - | 0.138 | 0.255 | - | 0.134 | 0.258 |
| 46 | 0.133 | 0.142 | 0.277 | - | - | - | - | 0.138 | 0.254 | - | 0.133 | 0.257 |
| 47 | 0.132 | 0.141 | 0.277 | - | - | - | - | 0.137 | 0.254 | - | 0.133 | 0.257 |
| 48 | 0.131 | 0.141 | 0.277 | - | - | - | - | 0.137 | 0.254 | - | 0.132 | 0.257 |
| 49 | 0.131 | 0.140 | 0.276 | - | - | - | - | 0.136 | 0.253 | - | 0.132 | 0.257 |
| 50 | 0.130 | 0.140 | 0.276 | - | - | - | - | 0.136 | 0.253 | - | 0.131 | 0.256 |
| 51 | 0.129 | 0.140 | 0.276 | - | - | - | - | 0.135 | 0.253 | - | 0.131 | 0.256 |
| 52 | 0.128 | 0.139 | 0.276 | - | - | - | - | 0.135 | 0.252 | - | 0.130 | 0.256 |
| 53 | 0.128 | 0.139 | 0.276 | - | - | - | - | 0.134 | 0.252 | - | 0.129 | 0.256 |
| 54 | 0.127 | 0.138 | 0.276 | - | - | - | - | 0.134 | 0.252 | - | 0.129 | 0.256 |
| 55 | 0.126 | 0.138 | 0.275 | - | - | - | - | 0.133 | 0.251 | - | 0.128 | 0.255 |
| 56 | 0.126 | 0.137 | 0.275 | - | - | - | - | 0.133 | 0.251 | - | 0.128 | 0.255 |
| 57 | 0.125 | 0.137 | 0.275 | - | - | - | - | 0.132 | 0.251 | - | 0.127 | 0.255 |
| 58 | 0.124 | 0.136 | 0.275 | - | - | - | - | 0.132 | 0.251 | - | 0.126 | 0.255 |
| 59 | 0.123 | 0.135 | 0.275 | - | - | - | - | 0.131 | 0.250 | - | 0.126 | 0.255 |
| 60 | 0.123 | - | 0.275 | - | - | - | - | 0.131 | 0.250 | - | 0.125 | 0.254 |

Table B.4: Einstein coefficients A of laser transitions of $^{12}\text{C}^{18}\text{O}$, s^{-1}

| J | Regular | | | Sequence | | | Hot-e | | | Hot-f | | |
|-----|---------|-------|-------|----------|-------|-------|-------|-----|-------|-------|-------|-------|
| | 10P | 10R | 9R | 10P | 10R | 9R | 10P | 10R | 9P | 10P | 10R | 9R |
| 0 | - | 0.073 | - | 0.234 | - | - | - | - | - | - | - | - |
| 1 | - | - | - | - | [0.2] | [0.7] | - | - | - | - | - | - |
| 2 | 0.146 | 0.094 | 0.466 | 0.301 | - | [0.7] | - | - | - | - | - | 0.243 |
| 3 | - | - | - | - | [0.2] | [0.7] | - | - | 0.337 | - | - | - |
| 4 | 0.125 | 0.100 | 0.398 | 0.321 | - | - | - | - | - | - | 0.105 | 0.338 |
| 5 | - | - | - | - | [0.2] | [0.7] | - | - | - | - | - | 0.280 |
| 6 | 0.119 | 0.103 | 0.379 | 0.330 | - | [0.7] | - | - | - | 0.127 | 0.111 | 0.334 |
| 7 | - | - | - | - | [0.2] | [0.7] | - | - | - | - | - | - |
| 8 | 0.116 | 0.104 | 0.368 | 0.337 | - | [0.7] | - | - | - | - | - | 0.301 |
| 9 | - | - | - | - | [0.2] | [0.7] | - | - | - | - | - | - |
| 10 | 0.114 | 0.105 | 0.363 | 0.340 | - | [0.7] | - | - | - | 0.125 | 0.113 | 0.330 |
| 11 | - | - | - | - | [0.2] | [0.7] | - | - | - | 0.124 | 0.115 | 0.327 |
| 12 | 0.112 | 0.106 | 0.360 | 0.343 | - | [0.7] | - | - | - | - | - | - |
| 13 | - | - | - | - | [0.2] | [0.7] | - | - | - | 0.123 | 0.116 | 0.324 |
| 14 | 0.111 | 0.106 | 0.356 | 0.347 | - | [0.7] | - | - | - | - | - | - |
| 15 | - | - | - | - | [0.2] | [0.7] | - | - | - | 0.122 | 0.117 | 0.322 |
| 16 | 0.110 | 0.107 | 0.353 | 0.349 | - | [0.7] | - | - | - | - | - | - |
| 17 | - | - | - | - | [0.2] | [0.7] | - | - | - | 0.121 | 0.117 | 0.320 |
| 18 | 0.109 | 0.107 | 0.351 | 0.351 | - | [0.7] | - | - | - | - | - | - |
| 19 | - | - | - | - | [0.2] | [0.7] | - | - | - | 0.120 | 0.118 | 0.318 |
| 20 | 0.108 | 0.107 | 0.349 | 0.353 | - | [0.7] | - | - | - | - | - | - |
| 21 | - | - | - | - | [0.2] | [0.7] | - | - | - | 0.119 | 0.118 | 0.317 |
| 22 | 0.108 | 0.107 | 0.348 | 0.355 | - | [0.7] | - | - | - | - | - | - |
| 23 | - | - | - | - | [0.2] | [0.7] | - | - | - | 0.119 | 0.118 | 0.315 |
| 24 | 0.107 | 0.107 | 0.346 | 0.357 | - | [0.7] | - | - | - | - | - | - |
| 25 | - | - | - | - | [0.2] | [0.7] | - | - | - | 0.118 | 0.118 | 0.314 |
| 26 | 0.106 | 0.107 | 0.346 | 0.359 | - | [0.7] | - | - | - | - | - | - |
| 27 | - | - | - | - | [0.2] | [0.7] | - | - | - | 0.117 | 0.118 | 0.313 |
| 28 | 0.105 | 0.107 | 0.343 | 0.360 | - | [0.7] | - | - | - | - | - | - |
| 29 | - | - | - | - | [0.2] | [0.7] | - | - | - | 0.116 | 0.118 | 0.312 |
| 30 | 0.105 | 0.107 | 0.342 | 0.362 | - | [0.7] | - | - | - | - | - | - |
| 31 | - | - | - | - | [0.2] | [0.7] | - | - | - | 0.116 | 0.118 | 0.311 |
| 32 | 0.104 | 0.106 | 0.341 | 0.364 | - | [0.7] | - | - | - | - | - | - |
| 33 | - | - | - | - | [0.2] | [0.7] | - | - | - | 0.115 | 0.118 | 0.310 |
| 34 | 0.103 | 0.106 | 0.340 | 0.365 | - | [0.7] | - | - | - | - | - | - |
| 35 | - | - | - | - | [0.2] | [0.7] | - | - | - | 0.114 | - | 0.309 |
| 36 | 0.102 | 0.106 | 0.340 | 0.367 | - | [0.7] | - | - | - | - | - | - |
| 37 | - | - | - | - | [0.2] | [0.7] | - | - | - | - | - | - |
| 38 | 0.101 | 0.105 | 0.339 | 0.369 | - | [0.7] | - | - | - | - | - | - |
| 39 | - | - | - | - | [0.2] | [0.7] | - | - | - | - | - | - |
| 40 | 0.100 | 0.104 | 0.338 | 0.370 | - | [0.7] | - | - | - | - | - | - |
| 41 | - | - | - | - | [0.2] | [0.7] | - | - | - | - | - | - |
| 42 | 0.100 | 0.104 | 0.337 | 0.372 | - | [0.7] | - | - | - | - | - | - |
| 43 | - | - | - | - | [0.2] | [0.7] | - | - | - | - | - | - |
| 44 | 0.098 | 0.104 | 0.336 | 0.373 | - | [0.7] | - | - | - | - | - | - |
| 45 | - | - | - | - | [0.2] | [0.7] | - | - | - | - | - | - |
| 46 | 0.097 | 0.103 | 0.335 | 0.375 | - | [0.7] | - | - | - | - | - | - |
| 47 | - | - | - | - | [0.2] | [0.7] | - | - | - | - | - | - |
| 48 | 0.096 | 0.103 | 0.335 | 0.376 | - | [0.7] | - | - | - | - | - | - |
| 49 | - | - | - | - | [0.2] | [0.7] | - | - | - | - | - | - |
| 50 | 0.095 | 0.102 | 0.333 | 0.378 | - | [0.7] | - | - | - | - | - | - |
| 51 | - | - | - | - | [0.2] | [0.7] | - | - | - | - | - | - |
| 52 | 0.095 | 0.101 | 0.333 | 0.378 | - | [0.7] | - | - | - | - | - | - |
| 53 | - | - | - | - | [0.2] | [0.7] | - | - | - | - | - | - |
| 54 | 0.093 | 0.100 | 0.332 | 0.381 | - | [0.7] | - | - | - | - | - | - |
| 55 | - | - | - | - | [0.2] | [0.7] | - | - | - | - | - | - |
| 56 | 0.092 | 0.099 | 0.331 | 0.382 | - | [0.7] | - | - | - | - | - | - |
| 57 | - | - | - | - | [0.2] | [0.7] | - | - | - | - | - | - |
| 58 | - | - | 0.331 | 0.384 | - | [0.7] | - | - | - | - | - | - |
| 59 | - | - | - | - | [0.2] | [0.7] | - | - | - | - | - | - |
| 60 | - | - | 0.331 | - | - | - | - | - | - | - | - | - |

Table B.5: Einstein coefficients A of laser transitions of '636' CO₂, s⁻¹

| J | Regular | | | Sequence | | | Hot-e | | | Hot-f | | |
|-----|---------|-------|-------|----------|-------|-------|-------|-------|-------|-------|-------|-------|
| | 10P | 10R | 9P | 9R | 10P | 10R | 9P | 9R | 10P | 10R | 9P | 9R |
| 0 | - | 0.138 | - | 0.072 | - | - | - | - | - | - | - | - |
| 1 | - | - | - | - | 0.833 | 0.335 | - | 0.158 | - | - | - | - |
| 2 | 0.276 | 0.178 | 0.143 | 0.093 | - | - | - | 0.106 | - | 0.134 | 0.124 | 0.095 |
| 3 | - | - | - | - | 0.500 | 0.374 | 0.235 | 0.176 | 0.188 | 0.147 | 0.132 | 0.105 |
| 4 | 0.237 | 0.190 | 0.122 | 0.099 | - | - | - | - | - | - | - | - |
| 5 | - | - | - | - | 0.462 | 0.389 | 0.217 | 0.184 | 0.187 | 0.158 | 0.131 | 0.113 |
| 6 | 0.225 | 0.195 | 0.116 | 0.102 | - | - | - | - | - | - | - | - |
| 7 | - | - | - | - | 0.447 | 0.397 | 0.209 | 0.188 | 0.185 | 0.164 | 0.129 | 0.117 |
| 8 | 0.219 | 0.198 | 0.113 | 0.104 | - | - | - | - | - | - | - | - |
| 9 | - | - | - | - | 0.438 | 0.403 | 0.205 | 0.191 | 0.183 | 0.167 | 0.128 | 0.120 |
| 10 | 0.215 | 0.200 | 0.111 | 0.105 | - | - | - | - | - | - | - | - |
| 11 | - | - | - | - | 0.431 | 0.406 | 0.202 | 0.194 | 0.181 | 0.169 | 0.126 | 0.121 |
| 12 | 0.213 | 0.202 | 0.110 | 0.107 | - | - | - | - | - | - | - | - |
| 13 | - | - | - | - | 0.428 | 0.409 | 0.200 | 0.196 | 0.180 | 0.170 | 0.125 | 0.124 |
| 14 | 0.210 | 0.203 | 0.109 | 0.108 | - | - | - | - | - | - | - | - |
| 15 | - | - | - | - | 0.422 | 0.413 | 0.199 | 0.198 | 0.179 | 0.170 | 0.124 | 0.125 |
| 16 | 0.209 | 0.204 | 0.108 | 0.109 | - | - | - | - | - | - | - | - |
| 17 | - | - | - | - | 0.419 | 0.414 | 0.198 | 0.200 | 0.178 | 0.171 | 0.124 | 0.125 |
| 18 | 0.207 | 0.204 | 0.108 | 0.110 | - | - | - | - | - | - | - | - |
| 19 | - | - | - | - | 0.415 | 0.415 | 0.197 | 0.201 | 0.176 | 0.172 | 0.123 | 0.127 |
| 20 | 0.206 | 0.205 | 0.107 | 0.111 | - | - | - | - | - | - | - | - |
| 21 | - | - | - | - | 0.414 | 0.416 | 0.196 | 0.203 | 0.177 | 0.171 | 0.122 | 0.128 |
| 22 | 0.205 | 0.206 | 0.107 | 0.112 | - | - | - | - | - | - | - | - |
| 23 | - | - | - | - | 0.411 | 0.416 | 0.195 | 0.205 | 0.175 | 0.172 | 0.121 | 0.128 |
| 24 | 0.203 | 0.206 | 0.106 | 0.112 | - | - | - | - | - | - | - | - |
| 25 | - | - | - | - | 0.409 | 0.417 | 0.195 | 0.206 | 0.174 | 0.172 | 0.121 | 0.130 |
| 26 | 0.202 | 0.207 | 0.106 | 0.113 | - | - | - | - | - | - | - | - |
| 27 | - | - | - | - | 0.406 | 0.418 | 0.194 | 0.208 | 0.174 | 0.172 | 0.120 | 0.131 |
| 28 | 0.201 | 0.207 | 0.106 | 0.114 | - | - | - | - | - | - | - | - |
| 29 | - | - | - | - | 0.403 | 0.418 | 0.194 | 0.210 | 0.173 | 0.172 | 0.120 | 0.132 |
| 30 | 0.199 | 0.207 | 0.105 | 0.114 | - | - | - | - | - | - | - | - |
| 31 | - | - | - | - | 0.401 | 0.419 | 0.193 | 0.212 | 0.172 | 0.172 | 0.119 | 0.133 |
| 32 | 0.197 | 0.207 | 0.105 | 0.116 | - | - | - | - | - | - | - | - |
| 33 | - | - | - | - | 0.398 | 0.419 | 0.193 | 0.214 | 0.171 | 0.172 | 0.119 | 0.134 |
| 34 | 0.197 | 0.206 | 0.105 | 0.117 | - | - | - | - | - | - | - | - |
| 35 | - | - | - | - | 0.396 | 0.418 | 0.193 | 0.215 | 0.170 | 0.172 | 0.118 | 0.135 |
| 36 | 0.196 | 0.207 | 0.105 | 0.118 | - | - | - | - | - | - | - | - |
| 37 | - | - | - | - | 0.394 | 0.418 | 0.193 | 0.217 | 0.170 | 0.171 | 0.118 | 0.136 |
| 38 | 0.194 | 0.206 | 0.105 | 0.119 | - | - | - | - | - | - | - | - |
| 39 | - | - | - | - | 0.390 | 0.419 | 0.193 | 0.219 | 0.169 | 0.171 | 0.118 | 0.136 |
| 40 | 0.193 | 0.206 | 0.105 | 0.120 | - | - | - | - | - | - | - | - |
| 41 | - | - | - | - | 0.389 | 0.417 | 0.192 | 0.220 | 0.168 | 0.170 | 0.117 | 0.138 |
| 42 | 0.192 | 0.206 | 0.105 | 0.121 | - | - | - | - | - | - | - | - |
| 43 | - | - | - | - | 0.385 | 0.418 | - | - | 0.167 | 0.170 | 0.117 | 0.139 |
| 44 | 0.190 | 0.206 | 0.105 | 0.122 | - | - | - | - | - | - | - | - |
| 45 | - | - | - | - | - | - | - | - | - | - | - | - |
| 46 | 0.189 | 0.205 | 0.105 | 0.123 | - | - | - | - | - | - | - | - |
| 47 | - | - | - | - | - | - | - | - | - | - | - | - |
| 48 | 0.187 | 0.204 | 0.105 | 0.123 | - | - | - | - | - | - | - | - |
| 49 | - | - | - | - | - | - | - | - | - | - | - | - |
| 50 | 0.186 | 0.203 | 0.105 | 0.125 | - | - | - | - | - | - | - | - |
| 51 | - | - | - | - | - | - | - | - | - | - | - | - |
| 52 | 0.185 | 0.203 | 0.105 | 0.126 | - | - | - | - | - | - | - | - |
| 53 | - | - | - | - | - | - | - | - | - | - | - | - |
| 54 | 0.183 | 0.203 | 0.105 | 0.127 | - | - | - | - | - | - | - | - |
| 55 | - | - | - | - | - | - | - | - | - | - | - | - |
| 56 | 0.182 | 0.202 | 0.105 | 0.128 | - | - | - | - | - | - | - | - |
| 57 | - | - | - | - | - | - | - | - | - | - | - | - |
| 58 | 0.180 | 0.201 | 0.105 | 0.129 | - | - | - | - | - | - | - | - |
| 59 | - | - | - | - | - | - | - | - | - | - | - | - |
| 60 | 0.178 | - | 0.105 | - | - | - | - | - | - | - | - | - |

Table B.6: Einstein coefficients A of laser transitions of $^{638'}\text{CO}_2$, s^{-1}

| J | Regular | | | Sequence | | | Hot-e | | | Hot-f | | |
|-----|---------|-------|-------|----------|-----|----|-------|-------|-------|-------|-------|-------|
| | 10P | 10R | 9P | 10P | 10R | 9P | 10P | 10R | 9P | 10P | 10R | 9P |
| 0 | - | 0.117 | - | - | - | - | - | 0.093 | - | - | 0.093 | - |
| 1 | 0.350 | 0.141 | 0.315 | 0.106 | - | - | - | - | - | 0.155 | 0.118 | 0.098 |
| 2 | 0.233 | 0.151 | 0.210 | 0.127 | - | - | 0.155 | 0.118 | 0.163 | 0.125 | 0.118 | 0.125 |
| 3 | 0.210 | 0.157 | 0.189 | 0.136 | - | - | 0.165 | 0.129 | 0.173 | 0.137 | 0.130 | 0.137 |
| 4 | 0.199 | 0.160 | 0.179 | 0.145 | - | - | 0.166 | 0.136 | 0.174 | 0.144 | 0.136 | 0.174 |
| 5 | 0.194 | 0.163 | 0.174 | 0.147 | - | - | 0.164 | 0.139 | 0.172 | 0.148 | 0.140 | 0.173 |
| 6 | 0.190 | 0.165 | 0.171 | 0.149 | - | - | 0.164 | 0.142 | 0.171 | 0.151 | 0.142 | 0.171 |
| 7 | 0.187 | 0.166 | 0.168 | 0.151 | - | - | 0.163 | 0.144 | 0.170 | 0.154 | 0.144 | 0.170 |
| 8 | 0.185 | 0.167 | 0.166 | 0.152 | - | - | 0.162 | 0.145 | 0.169 | 0.155 | 0.146 | 0.169 |
| 9 | 0.183 | 0.168 | 0.165 | 0.153 | - | - | 0.161 | 0.147 | 0.168 | 0.157 | 0.147 | 0.168 |
| 10 | 0.182 | 0.169 | 0.164 | 0.154 | - | - | 0.160 | 0.147 | 0.167 | 0.158 | 0.148 | 0.167 |
| 11 | 0.181 | 0.170 | 0.163 | 0.155 | - | - | 0.159 | 0.148 | 0.166 | 0.159 | 0.149 | 0.167 |
| 12 | 0.180 | 0.170 | 0.162 | 0.156 | - | - | 0.158 | 0.149 | 0.165 | 0.160 | 0.150 | 0.166 |
| 13 | 0.179 | 0.171 | 0.161 | 0.157 | - | - | 0.157 | 0.150 | 0.164 | 0.161 | 0.150 | 0.165 |
| 14 | 0.178 | 0.171 | 0.161 | 0.158 | - | - | 0.156 | 0.151 | 0.163 | 0.162 | 0.151 | 0.165 |
| 15 | 0.177 | 0.172 | 0.160 | 0.158 | - | - | 0.155 | 0.151 | 0.162 | 0.163 | 0.151 | 0.164 |
| 16 | 0.176 | 0.172 | 0.160 | 0.159 | - | - | 0.154 | 0.151 | 0.161 | 0.164 | 0.151 | 0.164 |
| 17 | 0.176 | 0.172 | 0.159 | 0.160 | - | - | 0.153 | 0.152 | 0.163 | 0.165 | 0.152 | 0.164 |
| 18 | 0.175 | 0.173 | 0.159 | 0.160 | - | - | 0.152 | 0.151 | 0.162 | 0.166 | 0.152 | 0.163 |
| 19 | 0.174 | 0.173 | 0.158 | 0.161 | - | - | 0.151 | 0.151 | 0.161 | 0.166 | 0.152 | 0.163 |
| 20 | 0.174 | 0.173 | 0.158 | 0.161 | - | - | 0.150 | 0.151 | 0.161 | 0.166 | 0.151 | 0.166 |
| 21 | 0.173 | 0.173 | 0.158 | 0.162 | - | - | 0.149 | 0.151 | 0.161 | 0.167 | 0.151 | 0.167 |
| 22 | 0.173 | 0.173 | 0.157 | 0.162 | - | - | 0.148 | 0.151 | 0.161 | 0.167 | 0.151 | 0.167 |
| 23 | 0.172 | 0.173 | 0.157 | 0.163 | - | - | 0.147 | 0.151 | 0.160 | 0.168 | 0.151 | 0.168 |
| 24 | 0.171 | 0.173 | 0.157 | 0.164 | - | - | 0.146 | 0.151 | 0.160 | 0.169 | 0.151 | 0.168 |
| 25 | 0.171 | 0.173 | 0.157 | 0.164 | - | - | 0.145 | 0.151 | 0.160 | 0.169 | 0.151 | 0.169 |
| 26 | 0.170 | 0.173 | 0.156 | 0.165 | - | - | 0.144 | 0.151 | 0.159 | 0.170 | 0.151 | 0.169 |
| 27 | 0.170 | 0.173 | 0.156 | 0.165 | - | - | 0.143 | 0.151 | 0.159 | 0.170 | 0.151 | 0.169 |
| 28 | 0.169 | 0.173 | 0.156 | 0.166 | - | - | 0.142 | 0.151 | 0.159 | 0.171 | 0.151 | 0.170 |
| 29 | 0.168 | 0.173 | 0.156 | 0.166 | - | - | 0.141 | 0.151 | 0.158 | 0.171 | 0.149 | 0.171 |
| 30 | 0.168 | 0.173 | 0.156 | 0.167 | - | - | 0.140 | 0.151 | 0.158 | 0.172 | 0.149 | 0.171 |
| 31 | 0.167 | 0.173 | 0.155 | 0.168 | - | - | 0.139 | 0.151 | 0.158 | 0.172 | 0.148 | 0.172 |
| 32 | 0.167 | 0.173 | 0.155 | 0.168 | - | - | 0.138 | 0.151 | 0.157 | 0.173 | 0.148 | 0.173 |
| 33 | 0.166 | 0.173 | 0.155 | 0.169 | - | - | 0.137 | 0.151 | 0.157 | 0.173 | 0.147 | 0.173 |
| 34 | 0.166 | 0.173 | 0.155 | 0.169 | - | - | 0.136 | 0.151 | 0.157 | 0.174 | 0.147 | 0.173 |
| 35 | 0.165 | 0.173 | 0.155 | 0.170 | - | - | 0.135 | 0.151 | 0.157 | 0.175 | 0.146 | 0.174 |
| 36 | 0.164 | 0.173 | 0.155 | 0.171 | - | - | 0.134 | 0.151 | 0.157 | 0.175 | 0.146 | 0.175 |
| 37 | 0.164 | 0.173 | 0.155 | 0.171 | - | - | 0.133 | 0.151 | 0.156 | 0.176 | 0.146 | 0.175 |
| 38 | 0.163 | 0.172 | 0.155 | 0.172 | - | - | 0.132 | 0.150 | 0.156 | 0.176 | 0.145 | 0.176 |
| 39 | 0.162 | 0.172 | 0.155 | 0.172 | - | - | 0.131 | 0.150 | 0.156 | 0.177 | 0.145 | 0.176 |
| 40 | 0.162 | 0.172 | 0.154 | 0.173 | - | - | 0.130 | 0.150 | 0.156 | 0.177 | 0.144 | 0.177 |
| 41 | 0.161 | 0.172 | 0.154 | 0.174 | - | - | 0.129 | 0.150 | 0.155 | 0.178 | 0.144 | 0.177 |
| 42 | 0.161 | 0.172 | 0.154 | 0.174 | - | - | 0.128 | 0.150 | 0.155 | 0.178 | 0.143 | 0.178 |
| 43 | 0.160 | 0.171 | 0.154 | 0.175 | - | - | 0.127 | 0.149 | 0.155 | 0.179 | 0.142 | 0.178 |
| 44 | 0.159 | 0.171 | 0.154 | 0.175 | - | - | 0.126 | 0.149 | 0.155 | 0.179 | 0.142 | 0.179 |
| 45 | 0.159 | 0.171 | 0.154 | 0.176 | - | - | 0.125 | 0.149 | 0.155 | 0.180 | 0.141 | 0.179 |
| 46 | 0.158 | 0.170 | 0.154 | 0.177 | - | - | 0.124 | 0.149 | 0.154 | 0.181 | 0.141 | 0.180 |
| 47 | 0.157 | 0.170 | 0.154 | 0.177 | - | - | 0.123 | 0.148 | 0.154 | 0.181 | 0.140 | 0.181 |
| 48 | 0.157 | 0.170 | 0.154 | 0.178 | - | - | 0.122 | 0.148 | 0.154 | 0.182 | 0.140 | 0.181 |
| 49 | 0.156 | 0.169 | 0.154 | 0.179 | - | - | 0.121 | 0.148 | 0.154 | 0.182 | 0.139 | 0.182 |
| 50 | 0.155 | 0.169 | 0.154 | 0.179 | - | - | 0.120 | 0.147 | 0.154 | 0.183 | 0.139 | 0.182 |
| 51 | 0.154 | 0.169 | 0.154 | 0.180 | - | - | 0.119 | 0.147 | 0.154 | 0.183 | 0.138 | 0.183 |
| 52 | 0.154 | 0.168 | 0.154 | 0.181 | - | - | 0.118 | 0.147 | 0.153 | 0.184 | 0.138 | 0.184 |
| 53 | 0.153 | 0.168 | 0.154 | 0.181 | - | - | 0.117 | 0.147 | 0.153 | 0.184 | 0.137 | 0.184 |
| 54 | 0.152 | 0.167 | 0.154 | 0.182 | - | - | 0.116 | 0.146 | 0.153 | 0.185 | 0.136 | 0.185 |
| 55 | 0.152 | 0.167 | 0.154 | 0.183 | - | - | 0.115 | - | 0.153 | 0.186 | 0.136 | 0.186 |
| 56 | 0.151 | 0.167 | 0.154 | 0.184 | - | - | 0.114 | - | 0.153 | 0.186 | - | 0.186 |
| 57 | 0.150 | 0.166 | 0.154 | 0.184 | - | - | 0.113 | - | 0.153 | 0.187 | - | 0.187 |
| 58 | 0.149 | 0.166 | 0.154 | 0.185 | - | - | 0.112 | - | - | - | - | - |
| 59 | 0.149 | 0.165 | 0.154 | 0.186 | - | - | 0.111 | - | - | - | - | - |
| 60 | 0.148 | - | 0.155 | - | - | - | 0.110 | - | - | - | - | - |

Table B.7: Einstein coefficients A of laser transitions of '838' CO₂, s⁻¹

| J | Regular | | | Sequence | | | Hot-e | | | Hot-f | | |
|-----|---------|-------|-------|----------|-----|-----|-------|----|-----|-------|----|----|
| | 10P | 10R | 9P | 9R | 10P | 10R | 9P | 9R | 10P | 10R | 9P | 9R |
| 0 | - | - | - | - | - | - | - | - | - | - | - | - |
| 1 | - | - | - | - | - | - | - | - | - | - | - | - |
| 2 | - | - | - | - | - | - | - | - | - | - | - | - |
| 3 | - | - | - | - | - | - | - | - | - | - | - | - |
| 4 | - | - | - | - | - | - | - | - | - | - | - | - |
| 5 | - | - | - | - | - | - | - | - | - | - | - | - |
| 6 | 0.191 | 0.166 | 0.233 | 0.203 | - | - | - | - | - | - | - | - |
| 7 | - | - | - | - | - | - | - | - | - | - | - | - |
| 8 | 0.186 | 0.169 | 0.227 | 0.206 | - | - | - | - | - | - | - | - |
| 9 | - | - | - | - | - | - | - | - | - | - | - | - |
| 10 | 0.182 | 0.171 | 0.223 | 0.209 | - | - | - | - | - | - | - | - |
| 11 | - | - | - | - | - | - | - | - | - | - | - | - |
| 12 | 0.180 | 0.173 | 0.220 | 0.211 | - | - | - | - | - | - | - | - |
| 13 | - | - | - | - | - | - | - | - | - | - | - | - |
| 14 | 0.178 | 0.175 | 0.219 | 0.213 | - | - | - | - | - | - | - | - |
| 15 | - | - | - | - | - | - | - | - | - | - | - | - |
| 16 | 0.177 | 0.177 | 0.217 | 0.215 | - | - | - | - | - | - | - | - |
| 17 | - | - | - | - | - | - | - | - | - | - | - | - |
| 18 | 0.176 | 0.178 | 0.216 | 0.217 | - | - | - | - | - | - | - | - |
| 19 | - | - | - | - | - | - | - | - | - | - | - | - |
| 20 | 0.175 | 0.179 | 0.215 | 0.219 | - | - | - | - | - | - | - | - |
| 21 | - | - | - | - | - | - | - | - | - | - | - | - |
| 22 | 0.174 | 0.180 | 0.214 | 0.219 | - | - | - | - | - | - | - | - |
| 23 | - | - | - | - | - | - | - | - | - | - | - | - |
| 24 | 0.174 | 0.181 | 0.214 | 0.221 | - | - | - | - | - | - | - | - |
| 25 | - | - | - | - | - | - | - | - | - | - | - | - |
| 26 | 0.173 | 0.182 | 0.213 | 0.222 | - | - | - | - | - | - | - | - |
| 27 | - | - | - | - | - | - | - | - | - | - | - | - |
| 28 | 0.173 | 0.184 | 0.212 | 0.224 | - | - | - | - | - | - | - | - |
| 29 | - | - | - | - | - | - | - | - | - | - | - | - |
| 30 | 0.172 | 0.185 | 0.211 | 0.225 | - | - | - | - | - | - | - | - |
| 31 | - | - | - | - | - | - | - | - | - | - | - | - |
| 32 | 0.171 | 0.185 | 0.210 | 0.226 | - | - | - | - | - | - | - | - |
| 33 | - | - | - | - | - | - | - | - | - | - | - | - |
| 34 | - | - | - | - | - | - | - | - | - | - | - | - |
| 35 | - | - | - | - | - | - | - | - | - | - | - | - |
| 36 | - | - | - | - | - | - | - | - | - | - | - | - |
| 37 | - | - | - | - | - | - | - | - | - | - | - | - |
| 38 | - | - | - | - | - | - | - | - | - | - | - | - |
| 39 | - | - | - | - | - | - | - | - | - | - | - | - |
| 40 | - | - | - | - | - | - | - | - | - | - | - | - |
| 41 | - | - | - | - | - | - | - | - | - | - | - | - |
| 42 | - | - | - | - | - | - | - | - | - | - | - | - |
| 43 | - | - | - | - | - | - | - | - | - | - | - | - |
| 44 | - | - | - | - | - | - | - | - | - | - | - | - |
| 45 | - | - | - | - | - | - | - | - | - | - | - | - |
| 46 | - | - | - | - | - | - | - | - | - | - | - | - |
| 47 | - | - | - | - | - | - | - | - | - | - | - | - |
| 48 | - | - | - | - | - | - | - | - | - | - | - | - |
| 49 | - | - | - | - | - | - | - | - | - | - | - | - |
| 50 | - | - | - | - | - | - | - | - | - | - | - | - |
| 51 | - | - | - | - | - | - | - | - | - | - | - | - |
| 52 | - | - | - | - | - | - | - | - | - | - | - | - |
| 53 | - | - | - | - | - | - | - | - | - | - | - | - |
| 54 | - | - | - | - | - | - | - | - | - | - | - | - |
| 55 | - | - | - | - | - | - | - | - | - | - | - | - |
| 56 | - | - | - | - | - | - | - | - | - | - | - | - |
| 57 | - | - | - | - | - | - | - | - | - | - | - | - |
| 58 | - | - | - | - | - | - | - | - | - | - | - | - |
| 59 | - | - | - | - | - | - | - | - | - | - | - | - |
| 60 | - | - | - | - | - | - | - | - | - | - | - | - |

Appendix C

Properties of optical materials

The following expressions and values for linear (n_0) and nonlinear (n_2) refractive indexes are used in the program (wavelength λ in the dispersion formulas must be expressed in μm):

AgBr

$$n_0 = \sqrt{3.860 + \frac{0.8677\lambda^2}{\lambda^2 - 0.3211^2} + \frac{21.61\lambda^2}{\lambda^2 - 254.2^2}} \quad (\lambda = 0.495\text{--}12.67 \mu\text{m}) \text{ - Fit of data from [24] and [25]}$$
$$n_2 = 1 \times 10^{-19} \text{ m}^2/\text{W at } 9.2 \mu\text{m} \text{ - Preliminary estimate}$$

AgCl

$$n_0 = \sqrt{4.00804 + \frac{0.079086}{\lambda^2 - 0.04584} - 0.00085111\lambda^2 - 0.00000019762\lambda^4} \quad (\lambda = 0.578\text{--}20.6 \mu\text{m}) \text{ [26]}$$
$$n_2 = 1.7 \times 10^{-19} \text{ m}^2/\text{W at } 9.2 \mu\text{m} \text{ - Preliminary estimate}$$

AMTIR1 (IRG 22)

$$n_0 = \sqrt{3.4834 + \frac{2.8203\lambda^2}{\lambda^2 - 0.1352} + \frac{0.9773\lambda^2}{\lambda^2 - 1420.7}} \quad (\lambda = 0.8\text{--}15.5 \mu\text{m}) \text{ [27]}$$

BaF₂

$$n_0 = \sqrt{1.33973 + \frac{0.81070\lambda^2}{\lambda^2 - 0.10065^2} + \frac{0.19652\lambda^2}{\lambda^2 - 29.87^2} + \frac{4.52469\lambda^2}{\lambda^2 - 53.82^2}} \quad (\lambda = 0.15\text{--}15 \mu\text{m}) \text{ [28]}$$
$$n_2 = 1.7 \times 10^{-20} \text{ m}^2/\text{W at } 9.2 \mu\text{m} \text{ [29]}$$

CdTe

$$n_0 = \sqrt{1 + \frac{6.1977889\lambda^2}{\lambda^2 - 0.1005326} + \frac{3.2243821\lambda^2}{\lambda^2 - 5279.518}} \quad (\lambda = 6\text{--}22 \mu\text{m}) \text{ [30]}$$
$$n_2 = -2.95 \times 10^{-17} \text{ m}^2/\text{W at } 1.06 \mu\text{m} \text{ [31]}$$

CsI

$$n_0 = \sqrt{1.27587 + \frac{0.68689\lambda^2}{\lambda^2 - 0.130^2} + \frac{0.26090\lambda^2}{\lambda^2 - 0.147^2} + \frac{0.06256\lambda^2}{\lambda^2 - 0.163^2} + \frac{0.06527\lambda^2}{\lambda^2 - 0.177^2} + \frac{0.14991\lambda^2}{\lambda^2 - 0.185^2} + \frac{0.51818\lambda^2}{\lambda^2 - 0.206^2} + \frac{0.01918\lambda^2}{\lambda^2 - 0.218^2} + \frac{3.38229\lambda^2}{\lambda^2 - 161.29^2}}$$
$$(\lambda = 0.25\text{--}67 \mu\text{m}) \text{ [32]}$$
$$n_2 = 1.2 \times 10^{-19} \text{ m}^2/\text{W} \text{ - Preliminary estimate}$$

GaAs

$$n_0 = \sqrt{5.372514 + \frac{5.466742\lambda^2}{\lambda^2 - 0.4431307^2} + \frac{0.02429960\lambda^2}{\lambda^2 - 0.8746453^2} + \frac{1.957522\lambda^2}{\lambda^2 - 36.9166^2}} (\lambda = 0.97\text{--}17 \text{ }\mu\text{m}) [33]$$
$$n_2 = -3.26 \times 10^{-17} \text{ m}^2/\text{W at } 1.06 \text{ }\mu\text{m} [31]$$

Ge

$$n_0 = \sqrt{1 + \frac{0.4886331\lambda^2}{\lambda^2 - 1.393959} + \frac{14.5142535\lambda^2}{\lambda^2 - 0.1626427} + \frac{0.0091224\lambda^2}{\lambda^2 - 752.190}} (\lambda = 2\text{--}14 \text{ }\mu\text{m}) [34]$$
$$n_2 = 2.83 \times 10^{-17} \text{ m}^2/\text{W at } 10.6 \text{ }\mu\text{m} [31]$$

KBr

$$n_0 = \sqrt{1.39408 + \frac{0.79221\lambda^2}{\lambda^2 - 0.146^2} + \frac{0.01981\lambda^2}{\lambda^2 - 0.173^2} + \frac{0.15587\lambda^2}{\lambda^2 - 0.187^2} + \frac{0.17673\lambda^2}{\lambda^2 - 60.61^2} + \frac{2.06217\lambda^2}{\lambda^2 - 87.72^2}} (\lambda = 0.2\text{--}42 \text{ }\mu\text{m}) [32]$$

KCl

$$n_0 = \sqrt{1.26486 + \frac{0.30523\lambda^2}{\lambda^2 - 0.100^2} + \frac{0.41620\lambda^2}{\lambda^2 - 0.131^2} + \frac{0.18870\lambda^2}{\lambda^2 - 0.162^2} + \frac{2.6200\lambda^2}{\lambda^2 - 70.42^2}} (\lambda = 0.18\text{--}35 \text{ }\mu\text{m}) [32]$$
$$n_2 = 5.6 \times 10^{-20} \text{ m}^2/\text{W at } 1.06 \text{ }\mu\text{m} [31] \quad n_2 = 3.4 \times 10^{-20} \text{ m}^2/\text{W at } 9.2 \text{ }\mu\text{m} [29]$$

NaCl

$$n_0 = \sqrt{1.00055 + \frac{0.19800\lambda^2}{\lambda^2 - 0.050^2} + \frac{0.48398\lambda^2}{\lambda^2 - 0.100^2} + \frac{0.38696\lambda^2}{\lambda^2 - 0.128^2} + \frac{0.25998\lambda^2}{\lambda^2 - 0.158^2} + \frac{0.08796\lambda^2}{\lambda^2 - 40.50^2} + \frac{3.17064\lambda^2}{\lambda^2 - 60.98^2} + \frac{0.30038\lambda^2}{\lambda^2 - 120.34^2}} (\lambda = 0.2\text{--}30 \text{ }\mu\text{m}) [32]$$
$$n_2 = 4.38 \times 10^{-20} \text{ m}^2/\text{W at } 1.06 \text{ }\mu\text{m} [31] \quad n_2 = 3.5 \times 10^{-20} \text{ m}^2/\text{W at } 9.2 \text{ }\mu\text{m} [29]$$

Si

$$n_0 = 3.41983 + \frac{0.159906}{\lambda^2 - 0.028} - 0.123109 \left(\frac{1}{\lambda^2 - 0.028} \right)^2 + 1.26878 \times 10^{-6} \lambda^2 - 1.95104 \times 10^{-9} \lambda^4$$
$$(\lambda = 2.44\text{--}25 \text{ }\mu\text{m}) [35]$$
$$n_2 = 1.0 \times 10^{-17} \text{ m}^2/\text{W at } 2.2 \text{ }\mu\text{m} [36]$$

SiO₂

$$n_0 = \sqrt{1 + \frac{0.6961663\lambda^2}{\lambda^2 - 0.0684043^2} + \frac{0.4079426\lambda^2}{\lambda^2 - 0.1162414^2} + \frac{0.8974794\lambda^2}{\lambda^2 - 9.896161^2}} (\lambda = 0.21\text{--}6.7 \text{ }\mu\text{m}) [37]$$
$$n_2 = 3.29 \times 10^{-20} \text{ m}^2/\text{W at } 1.06 \text{ }\mu\text{m} [31]$$

ZnS

$$n_0 = \sqrt{8.393 + \frac{0.14383}{\lambda^2 - 0.2421^2} + \frac{4430.99}{\lambda^2 - 36.71^2}} (\lambda = 0.405\text{--}13 \text{ }\mu\text{m}) [38]$$
$$n_2 = 2.5 \times 10^{-19} \text{ m}^2/\text{W at } 9.2 \text{ }\mu\text{m} - \text{Preliminary estimate}$$

ZnSe

$$n_0 = \sqrt{1 + \frac{4.45813734\lambda^2}{\lambda^2 - 0.200859853^2} + \frac{0.467216334\lambda^2}{\lambda^2 - 0.391371166^2} + \frac{2.89566290\lambda^2}{\lambda^2 - 47.1362108^2}} (\lambda = 0.54\text{--}18.2 \text{ }\mu\text{m}) [39]$$
$$n_2 = 2.87 \times 10^{-18} \text{ m}^2/\text{W at } 1.06 \text{ }\mu\text{m} [31]$$

Air

Refractive index n_0 is calculated using Mathar's model for $\lambda = 7.5\text{--}14\text{ }\mu\text{m}$ [40]
 $n_2 = 3 \times 10^{-23}\text{ m}^2/\text{W}$ at $9.2\text{ }\mu\text{m}$ [41]

Appendix D

Selected formulas explained

Equation 4.4

Eq. 4.4 defines the fraction z_{jk} of discharge energy spent in inelastic collisions:

$$z_{jk} = 10^{16} \frac{y_j u_{jk} \omega_{jk}}{\left(\frac{\xi \mathcal{E}}{\mathcal{N}} \right) v_d}$$

where $y_j[-]$ is the relative concentration of a component in the gas mixture, $u_{jk}[\text{eV}]$ is the transferred energy per electron-molecule collision, collision rate constant $\omega_{jk}[\text{cm}^3 \cdot \text{s}^{-1}]$ divided by electron drift speed $v_d[\text{cm} \cdot \text{s}^{-1}]$ is the collision cross-section ($[\text{cm}^2]$), $\mathcal{E}[10^{-16} \text{V} \cdot \text{cm}^{-1}]$ is the electric field, $\xi[\text{eV} \cdot \text{V}^{-1}]$ is the energy gained by electron moved across an electric potential difference of 1 V, and $\mathcal{N}[\text{cm}^{-3}]$ is the total absolute concentration of the gas mixture.

The physical meaning of $\xi \mathcal{E}$ is the energy (in eV) gained by an electron after passing 1 cm in the electric field \mathcal{E} . By definition of electronvolt, $\xi = 1$ and is thus omitted in Eq. 4.4.

Pumping rate constants in equations 4.8 and 4.9

Pumping rate constant is the number of quanta added to a given vibrational mode per unit of time per molecule.

$$p_e = \frac{1}{E_v[\text{J}]} \times \frac{1}{N[\text{cm}^{-3}]n[-]y[-]} \times q[-]W[\text{J} \cdot \text{s}^{-1} \cdot \text{cm}^{-3}]$$

where E_v is the energy of the vibrational quanta: 4.665e-20 J (2349 cm^{-1}) for ν_3 mode of CO_2 (and roughly same for N_2 vibration), and 1.325e-20 J (667 cm^{-1}) for ν_2 mode; $N=2.7\text{e}19 \text{ cm}^{-3}$ is the density of gas molecules under normal conditions (1 bar, 273 K); q is the fraction of discharge energy deposited in the corresponding vibration; n is the correction factor for molecular density at the conditions different from 'normal'; y is the relative concentration of the gas in the mixture; W is the discharge power density.

Combining the constants and switching to kW/cm^3 for power density and μs^{-1} for the rate constants we get the formulas given in the model description:

$$p_{e4} = 0.8 \times 10^{-3} \frac{q_4}{ny_2} W(t); \quad p_{e3} = 0.8 \times 10^{-3} \frac{q_3}{ny_1} W(t); \quad p_{e2} = 2.8 \times 10^{-3} \frac{q_2}{ny_1} W(t);$$

Bibliography

- [1] M. Born and E. Wolf, *Principles of Optics: Electromagnetic Theory of Propagation, Interference and Diffraction of Light*. Cambridge University Press, 1999.
- [2] A. E. Siegman, *Lasers*. University Science Books, 1986.
- [3] J. Peatross and M. Ware, *Physics of Light and Optics*. Available at optics.byu.edu, 2015.
- [4] N. V. Karlov and Y. B. Konev, “High pressure pulsed CO₂ lasers”, in *Handbook on lasers*, A. M. Prokhorov, Ed., Moscow: Sovetskoe Radio, 1978 (in Russian).
- [5] T. Holstein, “Energy distribution of electrons in high frequency gas discharges”, *Phys. Rev.*, vol. 70, pp. 367–384, 1946. DOI: 10.1103/PhysRev.70.367.
- [6] W. L. Nighan, “Electron energy distributions and collision rates in electrically excited N₂, CO, and CO₂”, *Phys. Rev. A*, vol. 2, pp. 1989–2000, 1970. DOI: 10.1103/PhysRevA.2.1989.
- [7] R. D. Hake and A. V. Phelps, “Momentum-transfer and inelastic-collision cross sections for electrons in O₂, CO, and CO₂”, *Phys. Rev.*, vol. 158, pp. 70–84, 1967. DOI: 10.1103/PhysRev.158.70.
- [8] L. S. Frost and A. V. Phelps, “Rotational excitation and momentum transfer cross sections for electrons in H₂ and N₂ from transport coefficients”, *Phys. Rev.*, vol. 127, pp. 1621–1633, 1962. DOI: 10.1103/PhysRev.127.1621.
- [9] A. S. Biryukov, V. K. Konyukhov, A. I. Lukovnikov, and R. I. Serikov, “Relaxation of the vibrational energy of the (00⁰1) level of the CO₂ molecule”, *Sov. J. Exp. Theor. Phys.*, vol. 39, p. 610, 1974.
- [10] R. L. Taylor and S. Bitterman, “Survey of vibrational relaxation data for processes important in the CO₂-N₂ laser system”, *Rev. Mod. Phys.*, vol. 41, pp. 26–47, 1969. DOI: 10.1103/RevModPhys.41.26.
- [11] B. J. Feldman, “Short-pulse multiline and multiband energy extraction in high-pressure CO₂-laser amplifiers”, *IEEE J. Quant. Electron.*, vol. 9, pp. 1070–1078, 1973. DOI: 10.1109/JQE.1973.1077412.
- [12] H. C. Volkin, “Calculation of short-pulse propagation in a large CO₂-laser amplifier”, *J. Appl. Phys.*, vol. 50, pp. 1179–1188, 1979. DOI: 10.1063/1.326148.
- [13] R. C. Hilborn, “Einstein coefficients, cross sections, f values, dipole moments, and all that”, *arXiv:physics/0202029*, 2002.
- [14] W. J. Witteman, *The CO₂ Laser*. Berlin Heidelberg New York Tokyo: Springer-Verlag, 1987.
- [15] J. J. Lowke, A. V. Phelps, and B. W. Irwin, “Predicted electron transport coefficients and operating characteristics of CO₂-N₂-He laser mixtures”, *J. Appl. Phys.*, vol. 44, pp. 4664–4671, 1973. DOI: 10.1063/1.1662017.
- [16] Y. D. Oksyuk, “Excitation of the rotational levels of diatomic molecules by electron impact in the adiabatic approximation”, *Sov. J. Exp. Theor. Phys.*, vol. 22, pp. 873–881, 1966.
- [17] N. Chandra and P. G. Burke, “Rotational excitation cross sections for e[−]-N₂ scattering”, *J. Phys. B: At. Mol. Phys.*, vol. 6, pp. 2355–2357, 1973. DOI: 10.1088/0022-3700/6/11/030.
- [18] A. V. Phelps, “Rotational and vibrational excitation of molecules by low-energy electrons”, *Rev. Mod. Phys.*, vol. 40, pp. 399–410, 1968. DOI: 10.1103/RevModPhys.40.399.

- [19] G. J. Schulz, “Vibrational excitation of nitrogen by electron impact”, *Phys. Rev.*, vol. 125, pp. 229–232, 1962. DOI: 10.1103/PhysRev.125.229.
- [20] A. G. Engelhardt, A. V. Phelps, and C. G. Risk, “Determination of momentum transfer and inelastic collision cross sections for electrons in nitrogen using transport coefficients”, *Phys. Rev.*, vol. 135, A1566–A1574, 1964. DOI: 10.1103/PhysRev.135.A1566.
- [21] I. E. Gordon, L. S. Rothman, C. Hill, R. V. Kochanov, Y. Tan, P. F. Bernath, M. Birk, V. Boudon, A. Campargue, K. V. Chance, B. J. Drouin, J.-M. Flaud, R. R. Gamache, J. T. Hodges, D. Jacquemart, V. I. Perevalov, A. Perrin, K. P. Shine, M.-A. H. Smith, J. Tennyson, G. C. Toon, H. Tran, V. G. Tyuterev, A. Barbe, A. G. Császár, V. M. Devi, T. Furtenbacher, J. J. Harrison, J.-M. Hartmann, A. Jolly, T. J. Johnson, T. Karman, I. Kleiner, A. A. Kyuberis, J. Loos, O. M. Lyulin, S. T. Massie, S. N. Mikhailenko, N. Moazzen-Ahmadi, H. S. P. Müller, O. V. Naumenko, A. V. Nikitin, O. L. Polyansky, M. Rey, M. Rotger, S. W. Sharpe, K. Sung, E. Starikova, S. A. Tashkun, J. V. Auwera, G. Wagner, J. Wilzewski, P. Wcisło, S. Yu, and E. J. Zak, “The hitran2016 molecular spectroscopic database”, *J. Quant. Spectr. Rad. Transfer*, vol. 203, pp. 3–69, 2017. DOI: 10.1016/j.jqsrt.2017.06.038.
- [22] A. Maki, C. Chou, K. Evenson, L. Zink, and J. Shy, “Improved molecular constants and frequencies for the CO₂ laser from new high-j regular and hot-band frequency measurements”, *J. Mol. Spectr.*, vol. 167, pp. 211–224, 1994. DOI: 10.1006/jmsp.1994.1227.
- [23] C. Freed, “Status of CO₂ isotope lasers and their applications in tunable laser spectroscopy”, *IEEE J. Quant. Electron.*, vol. 18, pp. 1220–1228, 1982. DOI: 10.1109/JQE.1982.1071680.
- [24] H. Schröer, “Über die brechungsindizes einiger schwermetallhalogenide im sichtbaren und die berechnung von interpolationsformeln für den dispersionsverlauf”, *Z. Phys.*, vol. 67, no. 1-2, pp. 24–36, Jan. 1931. DOI: 10.1007/bf01391040. [Online]. Available: <https://doi.org/10.1007/bf01391040>.
- [25] D. E. McCarthy, “Refractive index measurements of silver bromide in the infrared”, *Appl. Opt.*, vol. 12, no. 2, p. 409, Feb. 1973. DOI: 10.1364/ao.12.000409. [Online]. Available: <https://doi.org/10.1364/ao.12.000409>.
- [26] L. W. Tilton, E. K. Plyler, and R. E. Stephens, “Refractive index of silver chloride for visible and infrared radiant energy”, *J. Opt. Soc. Am.*, vol. 40, no. 8, p. 540, Aug. 1950. DOI: 10.1364/josa.40.000540. [Online]. Available: <https://doi.org/10.1364/josa.40.000540>.
- [27] *SCHOTT IRG 22 product flyer*, Apr. 2017. [Online]. Available: <https://refractiveindex.info/download/data/2017/schott-infrared-chalcogenide-glasses-irg-22-english-us-11052017.pdf>.
- [28] H. H. Li, “Refractive index of alkaline earth halides and its wavelength and temperature derivatives”, *J. Phys. Chem. Ref. Data*, vol. 9, no. 1, pp. 161–290, Jan. 1980. DOI: 10.1063/1.555616. [Online]. Available: <https://doi.org/10.1063/1.555616>.
- [29] M. N. Polyanskiy, I. V. Pogorelsky, M. Babzien, R. Kupfer, K. L. Vodopyanov, and M. A. Palmer, “Post-compression of long-wave infrared 2 picosecond sub-terawatt pulses in bulk materials”, *Opt. Express*, vol. 29, no. 20, p. 31 714, Sep. 2021. DOI: 10.1364/oe.434238.
- [30] A. G. DeBell, E. L. Dereniak, J. Harvey, J. P. J. Nissley, A. Selvarajan, and W. L. Wolfe, “Cryogenic refractive indices and temperature coefficients of cadmium telluride from 6 μm to 22 μm ”, *Appl. Opt.*, vol. 18, pp. 3114–3115, 1979. DOI: 10.1364/AO.18.003114.
- [31] M. Sheik-Bahae, “Dispersion of bound electron nonlinear refraction in solids”, *IEEE J. Quant. Electron.*, vol. 27, pp. 1296–1309, 1991. DOI: 10.1109/3.89946.
- [32] H. H. Li, “Refractive index of alkali halides and its wavelength and temperature derivatives”, *J. Phys. Chem. Ref. Data*, vol. 5, pp. 329–528, 1976. DOI: 10.1063/1.555536.
- [33] T. Skauli, P. S. Kuo, K. L. Vodopyanov, T. J. Pinguet, O. Levi, L. A. Eyres, J. S. Harris, M. M. Fejer, L. B. B. Gerard, and E. Lallier, “Improved dispersion relations for GaAs and applications to nonlinear optics”, *J. Appl. Opt.*, vol. 94, pp. 6447–6455, 2003. DOI: 10.1063/1.1621740.

- [34] J. H. Burnett, S. G. Kaplan, E. Stover, and A. Phenis, “Refractive index measurements of ge”, P. D. LeVan, A. K. Sood, P. Wijewarnasuriya, and A. I. D’Souza, Eds., SPIE Optical Engineering + Applications, 2016, San Diego, California, United States, SPIE, Sep. 2016. DOI: 10.1117/12.2237978. [Online]. Available: <https://doi.org/10.1117/12.2237978>.
- [35] D. F. Edwards and E. Ochoa, “Infrared refractive index of silicon”, *Appl. Opt.*, vol. 19, pp. 4130–4131, 1980. DOI: 10.1364/AO.19.004130.
- [36] A. D. Bristow, N. Rotenberg, and H. M. van Driel, “Two-photon absorption and kerr coefficients of silicon for 850–2200 nm”, *Appl. Phys. Lett.*, vol. 90, p. 191 104, 2007. DOI: 10.1063/1.2737359.
- [37] I. H. Malitson, “Interspecimen comparison of the refractive index of fused silica*,y”, *J. Opt. Soc. Am.*, vol. 55, no. 10, p. 1205, Oct. 1965. DOI: 10.1364/josa.55.001205. [Online]. Available: <https://doi.org/10.1364/josa.55.001205>.
- [38] C. A. Klein, “Room-temperature dispersion equations for cubic zinc sulfide”, *Appl. Opt.*, vol. 25, no. 12, p. 1873, Jun. 1986. DOI: 10.1364/ao.25.001873. [Online]. Available: <https://doi.org/10.1364/ao.25.001873>.
- [39] B. Tatian, “Fitting refractive-index data with the Sellmeier dispersion formula”, *Appl. Opt.*, vol. 23, pp. 4477–4485, 1984. DOI: 10.1364/AO.23.004477.
- [40] R. J. Mathar, “Refractive index of humid air in the infrared: Model fits”, *J. Opt. A*, vol. 9, pp. 470–476, 2007. DOI: 10.1088/1464-4258/9/5/008.
- [41] M. N. Polyanskiy, M. Babzien, I. V. Pogorelsky, R. Kupfer, K. L. Vodopyanov, and M. A. Palmer, “Single-shot measurement of the nonlinear refractive index of air at 92 μm with a picosecond terawatt CO2 laser”, *Opt. Lett.*, vol. 46, no. 9, p. 2067, Apr. 2021. DOI: 10.1364/ol.423800.